UC Santa Barbara

UC Santa Barbara Previously Published Works

Title

A framework for the forensic-engineering assessment of reservoir operation during floods based on a new standard operation policy

Permalink

https://escholarship.org/uc/item/7j4221sp

Authors

Zarei, Manizhe

Bozorg-Haddad, Omid

Loáiciga, Hugo A

Publication Date

2023-09-01

DOI

10.1016/j.jhydrol.2023.129774

Peer reviewed

eScholarship.org Powered by the California Digital Library
University of California

Journal of Hydrology 624 (2023) 129774

Contents lists available at ScienceDirect

Journal of Hydrology

journal homepage: www.elsevier.com/locate/jhydrol

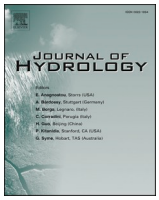

Research papers

A framework for the forensic-engineering assessment of reservoir operation during floods based on a new standard operation policy

Manizhe Zarei [a], Omid Bozorg-Haddad [a,*], Hugo A. Loáiciga [b]

[a] Department of Irrigation & Reclamation Engineering, College of Agriculture & Natural Resources, University of Tehran, Tehran, Iran
[b] Department of Geography, University of California, Santa Barbara, CA 93016-4060. USA

ARTICLE INFO

Keywords:
Forensic engineeringk
Flood control
Standard operation policy
Optimal reservoir operation
Ideal approach
Genetic algorithm

ABSTRACT

Floods inflict financial and human losses worldwide. The importance of assessing the effectiveness of flood management policies rises as the frequency and severity of floods increase. This study presents a novel forensic engineering framework for assessing the role of reservoir operation in achieving objectives under flood conditions. Specifically, this work develops two approaches, called the standard operation policy (SOP) and the ideal approach (IA) for the forensic assessment of reservoir-operation performance, which are compared with the historic management (HM) of reservoirs under flood conditions. This work introduces an innovative SOP for operation of reservoirs with the functions of flood control, meeting water demands, and hydropower generation. The genetic algorithm (GA) with the objective function of minimizing the maximum release from the most downstream reservoir in a multi-reservoir system is applied with the IA. The proposed framework is applied to evaluate the performance of the Seimare and Karkheh reservoirs system during floods in 2019 and 2020 in the Karkheh basin, Iran. The results show that in 2018–2019 and 2019–2020, on average, and under HM, the Seimare reservoir's and Karkheh reservoir's performance were respectively 28 and 68% worse than the SOP, and they were respectively 46 and 83% worse than the IA. This work's forensic methods contribute to the practice of flood mitigation by means of reservoir operation.

1. Introduction

Floods cause losses of life and property the world over (Diakakis et al., 2020; Van Pham, 2011). Structural and non-structural methods are implemented to mitigate floods (Bozorg-Haddad et al., 2021a; Dodangeh et al., 2020; Zarei et al., 2021a). Reservoirs are one of the structural measures built to protect against floods, even though complete protection against extreme floods is not always possible (Huang et al., 2022; Zhou et al., 2014). The recurrence of floods and the rising presence of people and property within floodplains has increased the role of reservoirs in flood control (Boulange et al., 2021; Haghizadeh et al., 2017). Flood control aims to ensure dam safety and reduce flood damage downstream of reservoirs (Luo et al., 2015).

The operation of flood control reservoirs is carried out in three stages: (1) prior to floods; (2) during the flood rising; and (3) post flood. Pre-releasing of reservoir storage prior to flood arrival promotes free storage to store floods (Kong et al., 2022; Lund and Guzman, 1999). Determining reservoir pre-release values has been a challenge for water resources planners and operators due to the uncertainty of reservoir inflows (Abdi et al., 2021) and meeting the conflicting objectives of flood control reservoirs (Hossain et al., 2019; Zhao et al., 2014). Meeting downstream water demands, flood control, and hydropower generation functions may be conflicting objectives of flood control reservoirs (Zarei et al., 2021a). During flood rising operators seek to alleviate the downstream flood peak by storing floods in reservoirs without allowing the water surface level to exceed the safety level of the dam (Connaughton et al., 2014). The stored flood water in the reservoir is released after a flood occurs abiding by the damage threshold (DT) to provide free storage for storing subsequent floods in the reservoir (Nilsson and Berggren, 2000; Shrestha and Kawasaki, 2020). Large reservoirs can play a beneficial role in flood mitigation, but if not properly operated they can intensify the peak flood in downstream areas or may lose a large volume of their storage due to excessively cautious water releases (Delpasand et al., 2021; Harmancioğlu, 1994).

The common approach to reservoir operation relies on the application of reservoir-operating rule curves (Karamouz et al., 2012; Srinivasan and Philipose, 1996; Srivastava and Awchi, 2009; Yang et al., 2021; Zolghadr-Asli et al., 2019). Rule curves are used as a guide to determine

* Corresponding author.
E-mail addresses: Zarei.Manizhe@ut.ac.ir (M. Zarei), OBHaddad@ut.ac.ir (O. Bozorg-Haddad), Hugo.Loaiciga@ucsb.edu (H.A. Loáiciga).

https://doi.org/10.1016/j.jhydrol.2023.129774
Received 20 September 2022; Received in revised form 30 May 2023; Accepted 2 June 2023
Available online 7 June 2023
0022-1694/© 2023 Published by Elsevier B.V.

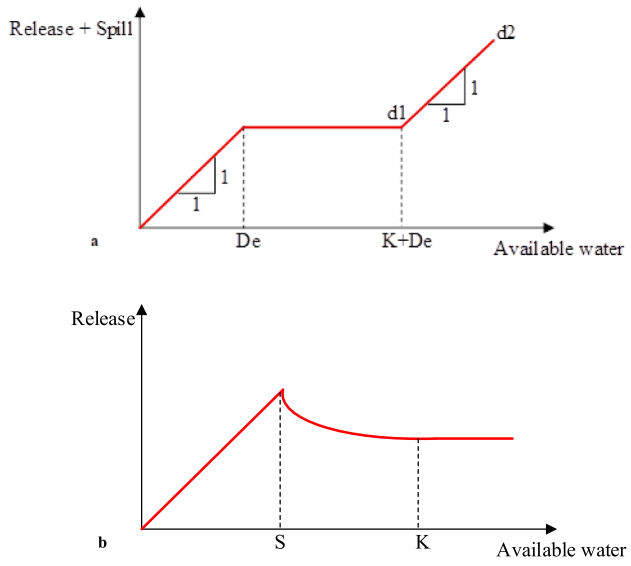

Fig. 1. The classic SOPs. a. SOP for meeting water demands (De and K denote water demand and reservoir capacity, respectively), b. SOP for a hydropower reservoir (S denotes the available reservoir water for generating hydropower).

the magnitude and timing of reservoir releases (Louks and Sigvaldason, 1981). The standard operation policy (SOP) is a simple and widely used operation policy that prescribes a pre-designed release schedule (Fig. 1a). Neelakantan and Sasireka (2013) proposed the SOP for hydropower reservoir operation (Fig. 1b). Despite available SOPs for the objectives of meeting downstream demands and hydropower generation no generic SOP has been so far proposed for operating flood control reservoirs. In addition, the SOP has not yet extended to cover the operation of multi-objective reservoirs. It is seen in Fig. 1a that the classic SOP is applied in reservoirs with free spillway following the 45° angle of the line d_1d_2. The classic SOP does not cover the operation of reservoirs with gated spillways. Another disadvantage of the SOP includes the lack of consideration of practical limitations in reservoir operation.

Unprecedented and prolonged precipitation in 2019 caused devastating floods in parts of Iran. This flood was one of the most severe floods in the last 70 years, especially in the country's southwestern regions, which caused environmental degradation and damage to building and agricultural lands, and at least 78 fatalities (Bozorg-Haddad et al., 2021a). Floods caused financial damage to Iran's southwestern regions in 2020 (Sadeghi et al., 2021). Many natural and/or human causes play a role in the occurrence of disasters. Discerning these causes and examining the origins and mechanisms in the formation of such extreme disasters is useful for providing solutions to mitigate their hazardous consequences (Zarei et al., 2021b).

Many prior investigations have dealt with several operational rules for large hydro-systems (Akbari-Alashti et al., 2014; Bahrami et al., 2018; Bozorg-Haddad et al., 2015; Bozorg-Haddad et al., 2016; Bozorg-Haddad and Mariño, 2011; Bozorg-Haddad et al., 2017; Bozorg-Haddad et al., 2009; Fallah-Mehdipour et al., 2011; Soltanjalili et al., 2011). However, few studies have considered testing the validity of the developed rules in real world settings after the occurrence of flood events. The forensic engineering approach consists in the application of engineering knowledge for assessing the role of natural and human causes in the occurrence of disasters (Carper, 2000; Noon, 2000; Zarei et al., 2021b). In recent decades, the forensic engineering approach has made a great contribution in identifying and clarifying the causes of disasters (Bronstert et al., 2018; Delpasand et al., 2021; Loáiciga, 2001). However, studies on proposing a framework for the forensic evaluation of reservoir performance during floods are scarce.

The necessity of providing a forensic engineering framework to evaluate reservoir performance under floods has gained relevance because of the significant increase in the frequency of major floods in recent decades and the large costs incurred on constructing and maintaining reservoirs. This study develops a framework to measure the role of reservoirs in mitigation or intensification of floods and meeting demands and generating the hydropower required by power supply networks. In this regard, the importance of proposing such framework is herein highlighted considering practical limitations to reservoir operation that are compared with the historical reservoir operation under flood conditions. This study presents a new SOP for the operation of multi-objective reservoirs under flood conditions. Practicality and simplicity of implementation are advantages of the proposed SOP that render it adaptable to forensic assessment criteria, and an effective alternative approach to guide operators during floods. Another approach that is included in this paper's forensic assessment framework is IA, which provides useful upper bounds on flood mitigation by reservoir operation assuming perfect knowledge of future inflows. This study develops novel forensic engineering criteria to guide accurate evaluation of reservoir's performance during flood conditions. The historical reservoir operation is compared with the SOP and IA by means of quantitative criteria guided by the forensic assessment framework presented in this study,.

2. Methodology

2.1. Forensic engineering: A disaster analysis approach

Forensic engineering is an approach developed in recent decades that applies engineering discipline to identify underlying factors that contributed to disasters to effectively mitigate such disasters in the future (Carper, 2000; Noon, 2000). In other words, this approach tackles two questions (Zarei et al., 2021b): What factors caused the disaster? and What measures must be taken to deal with such disasters in the future? Investigating the occurrence of disasters, forensic engineering addresses the need for a better understanding of their fundamental causes, which is essential to provide an alternative policy to mitigate and avoid future disasters. Forensic Hydrological Analysis (FDA) has emerged in recent years to detect the causes of hydrologic failures that inflicted damages in terms of loss of life and property; FDA is not restricted to extremes floods and drought, and it also studies water pollution, the drying up of lakes and rivers, and other calamities (Bronstert et al., 2018; Zarei et al., 2021b). Refer to Zarei et al. (2021b) for in-depth information about forensic engineering.

The forensic engineering framework proposed in this work involves assessing the HM by comparing it with the SOP's and the IA's performances. The scientific analysis of a system failure (e.g., during floods, drought, …) can be likened to a pyramid (Noon, 2000; Zarei et al., 2021b). The wider part of the pyramid is the evidence usable in forensic analysis. The forensic framework presented in this study assesses the HM as evidence and facts by implementing the SOP and IA. The top of the pyramid represents the position of the results and the causes of flood damages resulting from reservoir operation corresponding to the HM. Fig. 2 displays the flowchart of the forensic engineering framework presented in this work for evaluating the performance of HM during floods.

2.2. The proposed standard operation policy (SOP)

The proposed SOP focuses on practical reservoir operation with the objectives of flood control, meeting downstream water demands, and hydropower generation. The implementation of the SOP relies on the observed inflows to reservoirs. The following are the equations of the proposed SOP.

Reservoir water balance:

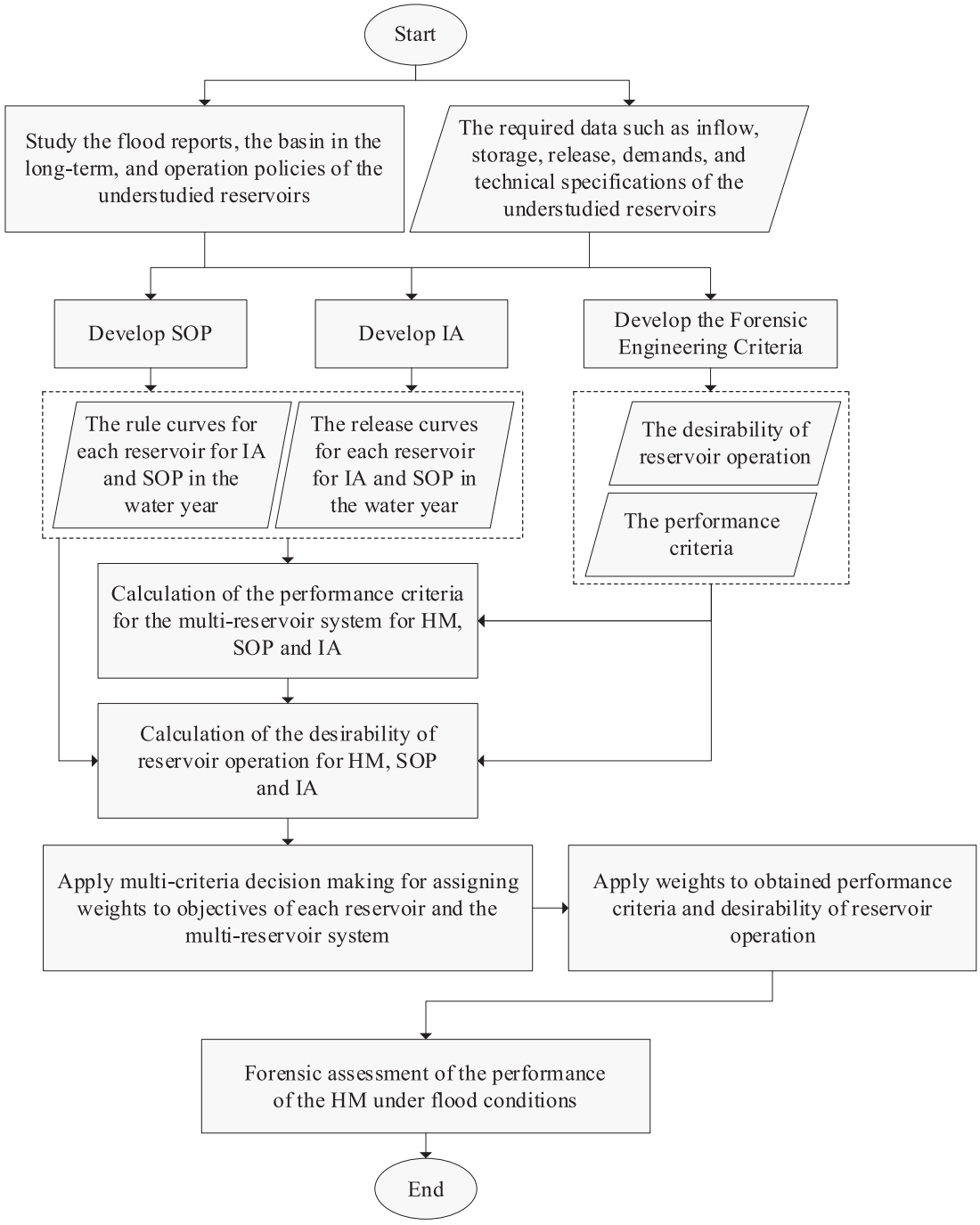

Fig. 2. Flowchart of the forensic framework for evaluating reservoir-operating performance during floods.

$$S_{i,t+1} = S_{i,t} + I_{i,t} + I'_{i-1,t} - E_{i,t} - I'_{i,t} i = 1, 2, ..., n \text{ and } t = 1, 2, ..., T \quad (1)$$

Regulated inflows:

$$I'_{i,t} = Rp_{i,t} + \sum_{j=1}^{m} R_{i,j,t} + Bo_{i,t} + Sf_{i,t} + Sg_{i,t} \quad (2)$$

Evaporation:

$$E_{i,t} = e_t \frac{(A_{i,t} + A_{i,t+1})}{2} \quad (3)$$

Reservoir water level:

$$H_{i,t} = G_i(S_{i,t}) \quad (4)$$

where n, t, T, $j = 1, 2, ..., m$, S, I, I', Bo, E, e, Rp, S_f, Sg, R, A, H, and G denote respectively the total number of reservoirs in a multi-reservoir system, with the reservoir index $i = 1, 2, \ldots, n$, the operation time step index, the total time steps in the operation horizon, the number of m reservoir gates, is the initial reservoir storage, the unregulated reservoir inflows, the release from the upstream reservoirs called the regulated inflow, the bottom outlet release, the evaporated water, the evaporation rate, the water release from the power plant, the spilled water from the reservoir's free spillway, the spilled water from the reservoir's gated spillway, the water released through other gates, the reservoir's water-surface area, the initial water level in the reservoir, and the level-storage reservoir function.

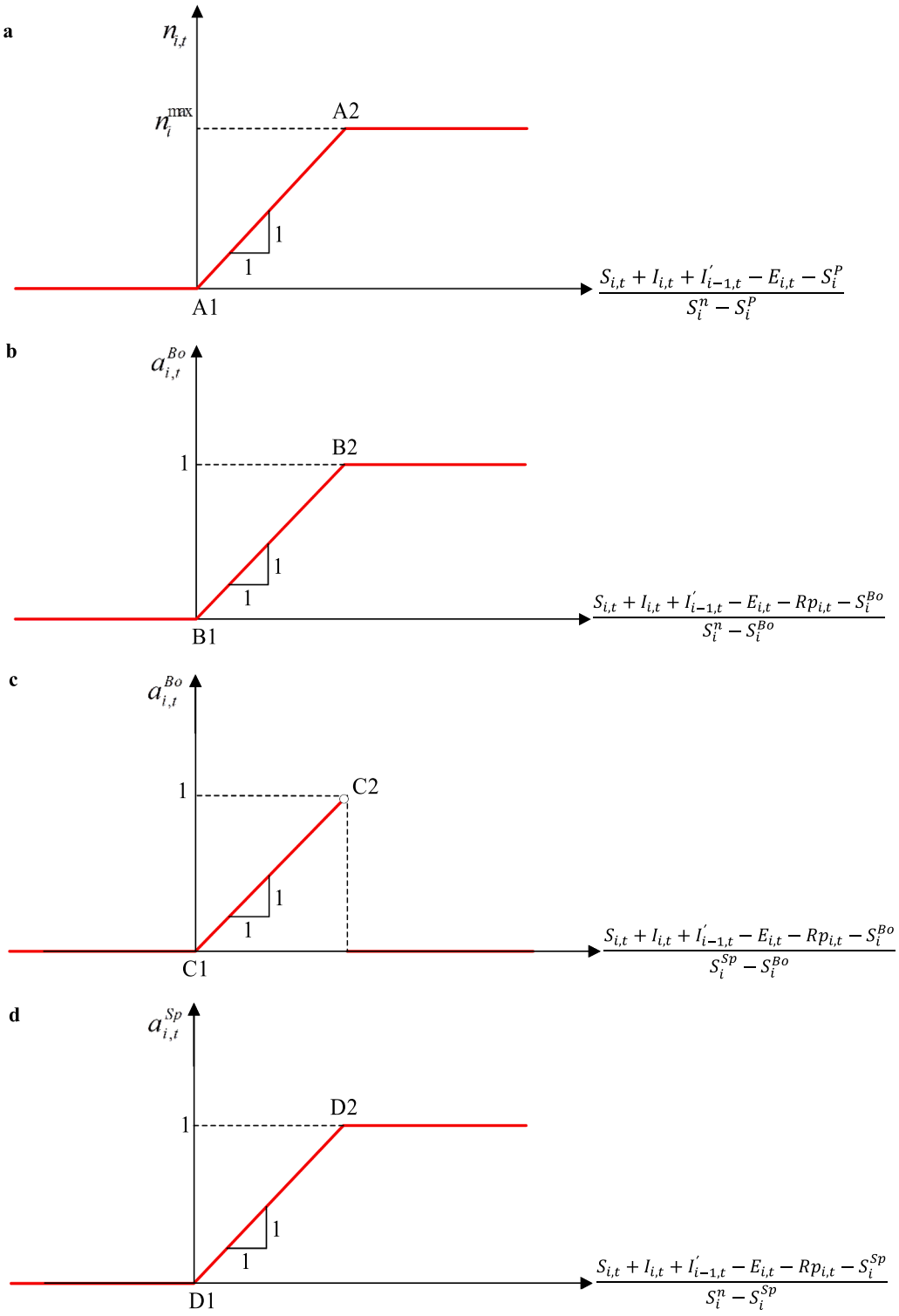

Fig. 3. Charts for determining parameters affecting reservoir release at time steps for the proposed SOP. a. The coefficient of the power plant performance, b. The opening of bottom outlet for reservoirs with free spillway; c. The opening of bottom outlet for reservoir with gated spillway, d. The opening of spillway gate. (S^P, S^{Bo}, S^{Sp} denote the minimum storage for powerplant performance, the storage at the bottom outlet level, the spill threshold storage, respectively.).

It is essential to measure the reservoir inflow and reservoir storage to decide about the timing and amounts of water release from the reservoirs in each time step. The SOP applies Eqs. (5) and (6) to quantify the inflow coefficient and the storage coefficient, respectively:

$$\alpha_{i,t} = \begin{cases} 0 & \text{if } \dfrac{(I_{i,t} + I'_{i-1,t} - NDT_i)}{(CDT_i - NDT_i)} < 0 \\ \dfrac{(I_{i,t} + I'_{i-1,t} - NDT_i)}{(CDT_i - NDT_i)} & \text{Otherwise} \end{cases} \quad (5)$$

$$\beta_{i,t} = \frac{S_{i,t} - S_i^{min}}{S_i^n - S_i^{min}} \quad (6)$$

in which α, NDT,CDT, β, $S^{\min}$ and S^n denote respectively the inflow coefficient, the no-downstream damage threshold, the severe downstream damage threshold, the storage coefficient, the minimum operating storage, and the normal reservoir storage.

The inflow coefficient calculated by Eq. (5) is assigned values between 0 and 1 for inflow between the NDT and CDT. It exceeds 1 for inflows greater than CDT. The reservoir storage coefficient takes values between 0 and 1 for storage between the minimum operating storage and the normal reservoir storage, and it is more than 1 for storage greater than the normal reservoir storage according to Eq. (6).

During reservoir operation in the flood season it may be necessary to pre-release water with minor damage in the remaining time before the flood peak to promote the required free storage to store future floods in the reservoir and prevent future large releases that may cause severe damages. In other words, it is sometimes crucial to accept the risk of releases in excess of NDT and to inflict downstream damages to forestall even greater downstream damages later. Therefore, the SOP considers the values of the reservoir inflow and storage coefficients to calculate the maximum reservoir release in each time step with Eq. (7).

$$O_{i,t}^{\max} = (1 + \min(\alpha_{i,t}, \beta_{i,t})) \times NDT_i \mathrm{i} = 1, 2, \ldots, \mathrm{n} \text{ and } \mathrm{t} = 1, 2, \ldots, \mathrm{T} \quad (7)$$

where $O_{i,t}^{\max}$ denotes the maximum release from reservoir i and time step t.

Whenever the water surface level is greater than or equal to the minimum level for powerplant performance the powerplant water release is given by Eq. (8), which in every time step is calculated to maximize meeting downstream demands and the power plant performance under the limitations imposed by the available reservoir storage and the calculated maximum reservoir output.

$$Rp_{i,t} = \begin{cases} Min(Max(De_{i,t}, Rp'_{i,t}), O_{i,t}^{\max}, WA_{i,t}) & \text{if } G_i(S_{i,t} + I_{i,t} + I'_{i-1,t} - E_{i,t}) \geqslant H_i^P \\ 0 & \text{Otherwise} \end{cases} \quad (8)$$

The target demand ($Rp'_{i,t}$) for hydropower generation is a function of the power plant performance coefficient ($n_{i,t}$)(in percentage) and the powerplant's net head ($Hnet_{i,t}^{Rp}$) calculated by Eq. (9) in each time step.

$$Rp'_{i,t} = \frac{86400 \times PPC_i \times n_{i,t} \times day}{\gamma_w \times g \times E'_i \times Hnet_{i,t}^{Rp}} \mathrm{i} = 1, 2, \ldots, \mathrm{n} \text{ and } \mathrm{t} = 1, 2, \ldots, \mathrm{T} \quad (9)$$

$$Hnet_{i,t}^{Rp} = G_i(S_{i,t} + I_{i,t} + I'_{i-1,t} - E_{i,t}) - Tw_{i,t} - H_{i,t}^{loss\ Rp} \mathrm{i} = 1, 2, \ldots, \mathrm{n} \text{ and } \mathrm{t} = 1, 2, \ldots, \mathrm{T} \quad (10)$$

in which De, WA, H^P, PPC, day, γ_w, g, E', Tw, and $H^{loss\ Rp}$ denote respectively the downstream water demand, the available reservoir water, the minimum water level for power plant performance, the installed power plant capacity, the number of days in each operation period, the volumetric weight of water equal to 1000 kg/m^3, the gravitational acceleration equal to 9.81 m/s^2, the power plant efficiency (in percentage), the water level at the power plant, and the head loss of the power plant.

In each time step the power plant performance coefficient is calculated with a linear function of the normalized storage between the minimum storage associated with the power plant performance and the normal storage, according to Fig. 3a (where S^P denotes the minimum storage for the power plant performance). It is seen in Fig. 3a that the power plant performance coefficient equals 0 when the storage is lower than the storage associated with the minimum power plant performance, it is between 0 and the maximum power plant's performance coefficients (MPPC) when the reservoir storage is less than the normal storage, and it equals MPPC when the reservoir storage is equal to or greater than the normal storage. The MPPC may not be necessarily 100% according to the performance characteristics of the power plant units in each time step.

The power plant's penstock is the first opened, if necessary, during reservoir operation, which releases reservoir water for meeting downstream water demand and attenuating floods, and to generate hydropower. The priority rule governing the opening of other gates is determined according to the reservoir operation policies. First priority is given to the power plant gates followed by opening the gates on the right or left sides of the reservoir (if available), as releasing from such gates does not increase the reservoir output and consequent downstream damages. It is noteworthy that the DTs on the right and left sides of the reservoir must be considered when releasing water from these gates to prevent damages. The value of the bottom outlet release ($Bo_{i,t}$) is given by Eq. (11) in reservoirs with a free spillway with no other controllable gates except the power plant and bottom outlet. Eq. (11) specifies that the water releases through the bottom outlet must meet the downstream demands subject to available reservoir storage whenever the power plant performance coefficient equals 0, and in time steps when the power plant performance coefficient is maximum the water release must be made through the bottom outlet to control flooding if the calculated maximum reservoir output is greater than the NDT. In this case the release from the bottom outlet is calculated subject to $O_{i,t}^{\max} - Rp_{i,t}$ and the available reservoir storage.

$$BO_{i,t} = \begin{cases} Min(De_{i,t}, WA_{i,t}) & \text{if } n_{i,t} = 0 \\ Min(BO'_{i,t}, (O_{i,t}^{\max} - Rp_{i,t})) & \text{if } n_{i,t} = n_{i,t}^{\max} \ \&\ O_{i,t}^{\max} > NDT_i \\ 0 & \text{Otherwise} \end{cases} \quad (11)$$

$$BO'_{i,t} = a_{i,t}^{BO} \times k_i^{BO} \sqrt{2g \times Hnet_{i,t}^{BO}} \times A_i^{BO} \in \mathrm{i} = 1, 2, \ldots, \mathrm{n} \text{ and } \mathrm{t} = 1, 2, \ldots, \mathrm{T} \quad (12)$$

$$Hnet_{i,t}^{BO} = G_i(S_{i,t} + I_{i,t} + I'_{i-1,t} - E_{i,t} - Rp_{i,t}) - H_i^{BO} - H_{i,t}^{loss\ BO} \mathrm{i} = 1, 2, \ldots, \mathrm{n} \text{ and } \mathrm{t} = 1, 2, \ldots, \mathrm{T} \quad (13)$$

in which $n^{\max}$,a^{Bo}, k^{Bo}, $Hnet^{Bo}$, A^{Bo}, H^{Bo}, $H^{loss\ Bo}$, and Bo' denote respectively the MPPC, the opening value of the bottom outlet (between 0 and 1), the bottom outlet efficiency, the bottom outlet's net head, the bottom outlet gate area, the bottom outlet level, the head loss of the bottom outlet, and is the target release from the bottom outlet under floods which is a function of its opening value and net head. In each time step opening value of the bottom outlet is calculated with a linear function of the normalized storage between the storage related to the bottom outlet level and the normal storage according to Fig. 3b (where S^{BO} denotes the storage at the bottom outlet level). It is seen in Fig. 3b that the opening of the bottom outlet when the storage falls below the bottom outlet equals 0, it is between 0 and 1 when the storage is between the bottom outlet level and normal storage (between points B_1 and B_2), and it equals 1 when the storage exceeds normal storage.

The water release from the bottom outlet in reservoirs with controllable gates of the power plant, bottom outlet and spillway, and

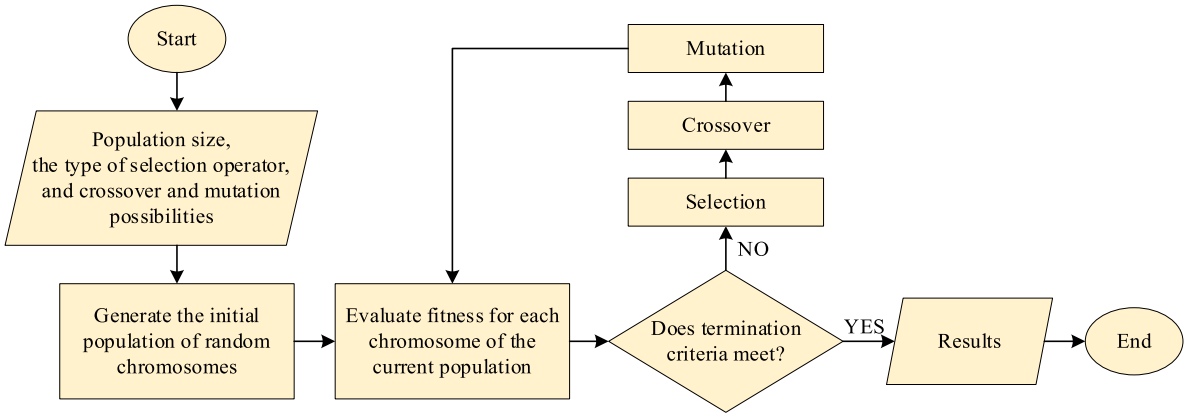

Fig. 4. Generalized flowchart of the GA.

storage lower than the spill threshold storage is given by Eq. (11). The opening value of the bottom outlet ($a_{i,t}^{Bo}$) for reservoirs with gated spillways is determined according to Fig. 3c (where S^{Sp} denotes the spill threshold storage). As Fig. 3c shows $a_{i,t}^{Bo}$ is between 0 and 1 when storage falls between the storage corresponding to the bottom outlet level and the spill threshold storage (between points C_1 and C_2), and it equals 0 when storage is equal to or greater than the spill threshold storage, in which case the gated spillway is opened rather than the bottom outlet, if necessary, because the increase in the net head of reservoir storage at the bottom outlet (for water levels more than the spill threshold level) may endanger dam safety by raising the speed of water outflow from the bottom outlet.

Eq. (14) shows how to calculate the reservoir spill in the free spillways ($Sf_{i,t}$). Reservoir spill occurs if the reservoir storage exceeds the normal storage. In time steps in which the MPPC occurs and the reservoir storage is lower than the normal storage and the calculated maximum reservoir output ($O^{\max}$) is more than the NDT the spill value ($Sg_{i,t}$) through the spillway gate is specified according to Eq. (15). In time steps when reservoir storage exceeds the normal storage surplus spills are executed to prevent overtopping the spillway gate.

$$Sf_{i,t} = \begin{cases} S_{i,t} + I_{i,t} + I'_{i-1,t} - E_{i,t} - Rp_{i,t} - BO_{i,t} - S_i^n & \text{if } S_{i,t} + I_{i,t} + I'_{i-1,t} - E_{i,t} - Rp_{i,t} - BO_{i,t} > S_i^n \\ 0 & \text{Otherwise} \end{cases} \tag{14}$$

$$Sg_{i,t} = \begin{cases} Min(Sg'_{i,t}, (O_{i,t}^{\max} - Rp_{i,t})) & \text{if} \begin{cases} n_{i,t} = n_{i,t}^{\max} \,\&\, O_{i,t}^{\max} > NDT_i \,\& \\ S_{i,t} + I_{i,t} + I'_{i-1,t} - E_{i,t} - Rp_{i,t} \leqslant S_i^n \end{cases} \\ S_{i,t} + I_{i,t} + I'_{i-1,t} - E_{i,t} - Rp_{i,t} - S_i^n & \text{if} \begin{cases} n_{i,t} = n_{i,t}^{\max} \,\& \\ S_{i,t} + I_{i,t} + I'_{i-1,t} - E_{i,t} - Rp_{i,t} > S_i^n \end{cases} \\ 0 & \text{Otherwise} \end{cases} \tag{15}$$

where

$$Sg'_{i,t} = a_{i,t}^{Sp} \times k_i^{Sp} \sqrt{2g \times Hnet_{i,t}^{Sp}} \times A_i^{Sp} \text{i} = 1, 2, \ldots, \text{n and t} = 1, 2, \ldots, \text{T} \tag{16}$$

$$Hnet_{i,t}^{Sp} = G_i(S_{i,t} + I_{i,t} + I'_{i-1,t} - E_{i,t} - Rp_{i,t}) - H_i^{Sp} - H_{i,t}^{loss\ Sp} \text{i} = 1, 2, \ldots, \text{n and t} = 1, 2, \ldots, \text{T} \tag{17}$$

in which a^{Sp}, k^{Sp}, $Hnet^{Sp}$, A^{Sp}, H^{Sp},$H^{loss\ Sp}$, and Sg' denote respectively the opening value of the spillway gate (between 0 and 1), the efficiency of the spillway gate, the gated spillway's net head, the spillway gate area, the spill threshold level, the head loss of the spillway gate, and the target release from the spillway gate under floods which is a function of its opening value and net head. The opening of the spillway gate at each time step is specified with a linear function of the normalized storage between the spill threshold storage and the normal storage according to Fig. 3d. As can be seen in Fig. 3d the opening of the spillway gate is 0 for storage lower than the spill threshold storage; it is between 0 and 1 when the reservoir storage is between the spill threshold storage and the normal storage, it equals 1 when the storage exceeds the normal storage.

2.2.1. *The generalized SOP for reservoirs without spillway gates*

Sometimes reservoirs' spillway gates are not installed because reservoir construction is not completed prior the flood season or because of attention given to development within flood plains and to prevent damages to the lands upstream of the reservoir. The SOP presented in this study is generalized for operating reservoirs without spillway gates during floods. Therefore, the spill threshold storage (S_i^{Sp}) replaces with the normal storage (S_i^n) in the previous Equations and Fig. 3, and the spill value is given by Eq. (18). In this case, closing the spillway chutes with stop logs (e.g., the gates constructed to be temporarily installed during the restoration of spillway gates, and which often are fewer in number than the number of spillway gates) during the flood season is an effective measure for increasing the reservoir capacity, preventing the spill the surplus reservoir storage, and providing additional protection downstream of reservoirs. Eq. (19) describes the status of stop logs for the proposed SOP. In time steps in which inflow coefficient exceeds 0 (i.e., the inflows are more than the NDT) and reservoir storage equals to the spill threshold storage, the spillway chutes are closed with stop logs, according to Eq. (19).

$$Sg_{i,t}=\begin{cases} S_{i,t}+I_{i,t}+I'_{i-1,t}-E_{i,t}-Rp_{i,t}-BO_{i,t}-S_i^{Sp} & \text{if } \begin{cases} S_{i,t}+I_{i,t}+I'_{i-1,t}-E_{i,t}-Rp_{i,t}-BO_{i,t}>S_i^{Sp}\,\& \\ \text{The spillway chutes are not closed with stop logs} \end{cases} \\ (S_{i,t}+I_{i,t}+I'_{i-1,t}-E_{i,t}-Rp_{i,t}-BO_{i,t}-S_i^{Sp})\times\dfrac{L_i-c_{i,t}}{L_i} & \text{if } \begin{cases} S_{i,t}+I_{i,t}+I'_{i-1,t}-E_{i,t}-Rp_{i,t}-BO_{i,t}>S_i^{Sp}\,\& \\ \text{The spillway chutes are closed with stop logs} \end{cases} \\ 0 & \text{if } S_{i,t}+I_{i,t}+I'_{i-1,t}-E_{i,t}-Rp_{i,t}-BO_{i,t}\leqslant S_i^{Sp} \end{cases} \tag{18}$$

$$\text{The stoplog status}=\begin{cases} \text{The spillway chutes are colsed with stop logs} & \text{if } \alpha_{i,t}>0\,\&\,S_{i,t}=S_i^{Sp} \\ \text{The spillway chutes are not colsed with stop logs} & \text{Otherwise} \end{cases} \tag{19}$$

where L denotes the number of the spillway chutes; and c is the number of closed spillway chutes with stop logs.

2.3. The ideal approach (IA)

The forensic assessment of the reservoirs' performance under floods requires investigating the infrastructure capacity for the flood mitigation. Besides errors in the operation of gates there may be other factors which could reduce the reservoirs' potential for mitigating flood damages within flood plains and sub-optimal reservoir design to cope with extreme flows. Therefore, it is imperative to develop an approach to analyze whether the flood-control infrastructure provided the capacity for flood attenuation. This work develops the ideal approach (IA) whereby knowledge of flood inflows to reservoirs are assumed known and thereby the focus is on objective of flood control, which enables the IA to measure the reservoir system's potential for flood mitigation. The IA calculates an upper bound to flood mitigation for the forensic analysis of HM's performance with respect to reservoir operation. The IA is herein developed by applying the optimal reservoir operation model (OROM), which is described below.

2.3.1. Optimal reservoir operation model (OROM)

The objective function is the minimization of the maximum release from the most downstream reservoir (the n-th reservoir in an n-reservoir system).

$$Z=Min\left[\underset{t=1}{\overset{T}{Max}}\left(Rp_{n,t}+\sum_{j=1}^{m}R_{n,j,t}+Bo_{n,t}+Sf_{n,t}+Sg_{n,t}\right)\right]t=1,2,\ldots,T \tag{20}$$

Subjected to:

Eqs. (1) to (4) are constraints, which are in addition to the constraints expressed by Eqs. (21) to (30):

Reservoir storage constraint:

$$0<S_i^{\min}\leqslant S_{i,t}\leqslant S_i^{\max} \tag{21}$$

where $S^{\max}$ denotes the maximum reservoir storage.

Power plant's constraints:

$$0\leqslant Rp_{i,t}\leqslant Rp_{i,t}^{\max} \tag{22}$$

$$0\leqslant n_{i,t}\leqslant n_{i,t}^{\max} \tag{23}$$

in which $Rp^{\max}$ denotes the maximum water release from the power plant.

Free spillway equation:

$$Sf_{i,t}\times\left(1-\frac{S_{i,t}+I_{i,t}+I'_{i-1,t}-E_{i,t}-Rp_{i,t}-Bo_{i,t}-\sum_{j=1}^{m}R_{i,j,t}}{S_i^n}\right)=0 \tag{24}$$

Gated spillway equation:

$$Sg_{i,t}=a_{i,t}^{Sp}\times k_i^{Sp}\sqrt{2g\times Hnet_{i,t}^{Sp}}\times A_i^{Sp} \tag{25}$$

$$0\leqslant Sg_{i,t}\leqslant Sg_{i,t}^{\max} \tag{26}$$

in which $Sg^{\max}$ denotes the maximum water release from the spillway gate.

Bottom outlet's constraints:

$$Bo_{i,t}=a_{i,t}^{Bo}\times k_i^{Bo}\sqrt{2g\times Hnet_{i,t}^{Bo}}\times A_i^{Bo} \tag{27}$$

$$0\leqslant Bo_{i,t}\leqslant Bo_{i,t}^{\max} \tag{28}$$

in which $Bo^{\max}$ denotes the maximum water release from the bottom outlet.

Other gates' constraint:

$$0\leqslant R_{i,j,t}\leqslant R_{i,j,t}^{\max} \tag{29}$$

in which $R^{\max}$ denotes the maximum water release from other reservoir gates.

Reservoir output constraint:

$$De_{i,t}\leqslant Rp_{i,t}+Bo_{i,t}+Sf_{i,t}+Sg_{i,t}+\sum_{j=1}^{m}R_{i,j,t} \tag{30}$$

2.3.2. The generalized OROM for reservoirs without spillway gates

The OROM involves a binary decision variable ($K_{i,t}$) for reservoirs in which spillway gates are not installed, which makes it capable of determining the smallest value of the fittness function in each time step by examining the options to close the spillway chutes or to leave them open. Eq. (31) describes the values of the binary decision variable in each time step. Eqs. (32) and (33) express additional constraints for the reservoirs.

$$K_{i,t}=\begin{cases} 1\text{if the spillwaychutes are closed with stop logs} \\ 0\text{Otherwise} \end{cases} \tag{31}$$

If $K_{i,t}=0$:

$$Sg_{i,t}\times\left(1-\frac{S_{i,t}+I_{i,t}+I'_{i-1,t}-E_{i,t}-Rp_{i,t}-Bo_{i,t}-\sum_{j=1}^{m}R_{i,j,t}}{S_i^{Sp}}\right)=0 \tag{32}$$

If $K_{i,t}=1$:

$$Sg_{i,t}=(S_{i,t}+I_{i,t}+I'_{i-1,t}-E_{i,t}-Rp_{i,t}-BO_{i,t}-S_i^{Sp})\times\frac{L_i-c_{i,t}}{L_i} \tag{33}$$

The GA (Holland, 1975) was implemented to solve the OROM embodied by Eqs. (1) to (4), Eqs. (20) to (33). The GA is described in the

next section.

2.3.3. Genetic algorithm

The GA is the most widely used Evolutionary Algorithm in the water resources planning and management literature (Chang and Chen, 1998; Che and Mays, 2015; Kim et al., 2006; Tegegne and Kim, 2020). The GA features a generational process cycle to achieve better solutions through evolution; evolution commences with a population of random chromosomes that provide all possible solutions for the first generation. The fitness of each chromosome of the population is evaluated, and multiple chromosomes are selected from the current population based on their fitness value, which is known as selection. Genetic operators (i.e. crossover and mutation) are used to modify the selected chromosomes to generate a new set of chromosomes that create the population for the next generation. These steps are repeated sequentially until the desired stopping criterion is fulfilled (Holland, 1975). Fig. 4 illustrates the general GA process. The reader can find more details about the GA in Holland (1975) and Golberg (1989).

In this study the GA was applied to solve the reservoir management model, as it has fast convergence to global optimal in high-dimensional and non-convex problems. In contrast, conventional optimization methods do not guarantee global optimal performance. For example, Yeh (1985) found Nonlinear Programming (NLP) methods could not solve large NLP reservoir management models due to the trap of infeasibility, or local solutions and slow convergence speed. Moreover, Dynamic Programming fails when the number of state variables and the scale of the problem increase and it succumbs to the curse of dimensionality (Ahmadianfar et al., 2017; Kumar and Yadav, 2020).

This work implemented the GA with population size between 200 and 300, crossover probability in the range 0.6–0.7, mutation probability in the range 0.001–0.01, and the stopping criterion featuring 1000 to 2000 iterations. The algorithmic parameters were selected based on the minimum of the fitness function. The selection operator of the Roulette Wheel (Fitness Proportionate Selection) (Holland, 1975) was used, which was superior to other selection operators with respect to optimal fitness values.

3. Forensic engineering criteria

Forensic analysis of reservoir performance requires numerical criteria to compare the results calculated with the SOP and IA with those corresponding to the HM. This study develops a novel forensic engineering criteria to evaluate the HM's operating performance.

3.1. Performance criteria

Three key probability-based performance criteria are reliability, resiliency, and vulnerability (Zolghadr-Asli et al., 2019). Reliability refers to how likely a reservoir system is to fail; resiliency measures how quickly it returns to a satisfactory state following a failure; and vulnerability quantifies the severity of failures over an operation horizon (Hashimoto et al., 1982). The numerical values of these criteria and the tradeoff among are helpful in the forensic assessment of reservoir operation. Generally, the higher the reliability and vulnerability of a reservoir system are, the more cautious policy an operating approach involves. For instance, in terms of flood control, an approach has the best performance in the mitigation of flood peak by assuring the reservoir's required free space to store floods and accepting the risk of releases with minor damage. Such an approach reduces vulnerability but also reduces reliability by incurring failures in some time steps.

This work develops reliability, resiliency and vulnerability criteria corresponding to the objectives of meeting water demands and hydropower generation by the operation of multi-reservoir systems. Refer to Delpasand et al. (2021) for in-depth information about the performance criteria for flood control. It is noteworthy that for a multi-reservoir system failure occurs when one or more of its components incur failure (Delpasand et al., 2021).

3.1.1. Performance criteria for meeting water demands

Meeting the water demands in each time step is the main criteria in this instance as stipulated below.

1. Reliability of meeting water demands in a multi-reservoir system

The reliability is calculated as follows:

$$Rel^{MD} = 1 - \frac{f_B^{MD}}{T}\ ,\ f_B^{MD} = \begin{cases} 1 & \sum_{i=1}^{n} f_i^{MD} \geqslant 1 \\ 0 & \sum_{i=1}^{n} f_i^{MD} < 1 \end{cases} \quad i = 1, 2, ..., n \tag{34}$$

where Rel^{MD}, f_B^{MD}, and f_i^{MD} denote the reliability of meeting water demands, the number of time steps with failure (i.e., the water demands are not met), and the number of time steps with failure in single reservoirs, respectively. The latter is given by:

$$f_i^{MD} = \sum_{t=1}^{T} a_{i,t}^{MD}\ ,\ a_{i,t}^{MD} = \begin{cases} 1 & Rp_{i,t} + Bo_{i,t} + Sf_{i,t} + Sg_{i,t} + \sum_{j=1}^{m} R_{i,j,t} < De_i \\ 0 & Rp_{i,t} + Bo_{i,t} + Sf_{i,t} + Sg_{i,t} + \sum_{j=1}^{m} R_{i,j,t} \geqslant De_i \end{cases} \quad \begin{matrix} i = 1, 2, ..., n \\ t = 1, 2, ..., T \end{matrix} \tag{35}$$

2. Resiliency to not-meeting water demands in a multi-reservoir system:

$$Res^{MD} = \frac{1}{\left(\frac{f_B^{MD}}{f_{S_B}^{MD}}\right)} \tag{36}$$

where Res^{MD} and $f_{S_B}^{MD}$ denote respectively the resiliency to not-meeting demands and the number of continuous time steps with failure for multi-reservoir systems.

3. Vulnerability to not-meeting demands in a multi-reservoir system:

$$Vul^{MD} = \frac{Max_{t=1}^{T}\left(\sum_{i=1}^{n} Max(De_{i,t} - (Rp_{i,t} + Bo_{i,t} + Sf_{i,t} + Sg_{i,t} + \sum_{j=1}^{m} R_{i,j,t}), 0)\right)}{\sum_{i=1}^{n} De_{i,t}} \quad \begin{matrix} \mathrm{i} = 1, 2, ..., \mathrm{n} \\ t = 1, 2, ..., T \end{matrix} \tag{37}$$

where Vul^{MD} denotes the vulnerability to not-meeting demands criterion of multi-reservoir systems.

3.1.2. Performance criteria for hydropower generation

Generating the PPC is the main criterion in this instance, and time steps with a generated hydropower lower than the PPC constitute a failure in hydropower reservoir systems.

any reservoir, and whose elements are the RMSEs with respect to the HM, SOP, and IA in the time steps with violations of the DTs, not meeting of water demands, and power generation being less than the PPC:

The elements of the matrix P are expressed by Eqs. (45) to (47):

$$P = \begin{array}{c} \\ \text{violation of DT} \\ \text{violation of meeting demands} \\ \text{violation of generating PPC} \end{array} \begin{array}{c} \begin{array}{ccc} \text{HM} & \text{SOP} & \text{IA} \end{array} \\ \begin{bmatrix} RMSE(1,1) & RMSE(1,2) & RMSE(1,3) \\ RMSE(2,1) & RMSE(2,2) & RMSE(2,3) \\ RMSE(3,1) & RMSE(3,2) & RMSE(3,3) \end{bmatrix} \end{array} \quad \begin{array}{l} i = 1,2,...,n \\ t = 1,2,...,T \end{array} \tag{44}$$

1. Reliability of hydropower generation in a multi-reservoir system:

$$Rel^{HP} = 1 - \frac{f_B^{HP}}{T}\ ,\ f_B^{HP} = \begin{cases} 1 & \sum_{i=1}^{n} f_i^{HP} \geqslant 1 \\ 0 & \sum_{i=1}^{n} f_i^{HP} < 1 \end{cases} \quad i = 1,2,...,n \tag{38}$$

in which Rel^{HP}, f_B^{HP}, and f_i^{HP} denote respectively the reliability of hydropower generation, the number of time steps with failure for multi-reservoir system, and the number of time steps with failure in single reservoirs, which is given by:

$$f_i^{HP} = \sum_{t=1}^{T} a_{i,t}^{HP}\ ,\ a_{i,t}^{HP} = \begin{cases} 1 & GP_{i,t} < PPC_i \\ 0 & GP_{i,t} = PPC_i \end{cases} \text{i} = 1,2,...,\text{n and t} = 1,2,...,\text{T} \tag{39}$$

where GP denotes the generated hydropower by each reservoir, which is given by:

$$GP_{i,t} = 0.01 \times n_{i,t} \times PPC_i \text{i} = 1,2,...,\text{n and t} = 1,2,...,\text{T} \tag{40}$$

2. Resiliency to generated hydropower less than the PPC in a multi-reservoir system:

$$Res^{HP} = \frac{1}{\left(\frac{f_B^{HP}}{f_{S_B}^{HP}}\right)} \tag{41}$$

where Res^{HP} denotes the resiliency to generated hydropower less than the PPC; and $f_{S_B}^{HP}$ represents the number of continuous time steps with failure in multi-reservoir systems.

3. Vulnerability to generated hydropower less than the PPC in a multi-reservoir system:

$$Vul^{HP} = \frac{\sum_{i=1}^{n}\sum_{t=1}^{T}\frac{(F_{i,t})^2}{\sum_{t=1}^{T}F_{i,t}}}{\sum_{i=1}^{n}PPC_i} \text{i} = 1,2,...,\text{n and t} = 1,2,...,\text{T} \tag{42}$$

where Vul^{HP} denotes the vulnerability to generated hydropower less than the PPC; and F represents the severity of failure for each reservoir, which is given by Equation (43).

$$F_{i,t} = \begin{cases} PPC_i - GP_{i,t} & if\ PPC_i - GP_{i,t} > 0 \\ 0 & if\ PPC_i - GP_{i,t} = 0 \end{cases} \text{i} = 1,2,...,\text{n and t} = 1,2,...,\text{T} \tag{43}$$

3.2. Desirability of reservoir operation (DRO)

The DRO evaluates reservoir management with respect to various functions such as flood control, meeting water demands, and hydropower generation. The DRO involves the P matrix that is constructed for

$$RMSE_{O_{i,t}>DT_i} = \sqrt{\frac{1}{T}\sum_{t=1}^{T}\left(Max(Rp_{i,t} + Bo_{i,t} + Sf_{i,t} + Sg_{i,t} + \sum_{j=1}^{m}R_{i,j,t} - DT_i, 0)\right)^2} \tag{45}$$

$$RMSE_{GP_{i,t}<PPC_i} = \sqrt{\frac{1}{T}\sum_{t=1}^{T}(PPC_i - GP_{i,t})^2} \tag{46}$$

$$RMSE_{O_{i,t}<De_{i,t}} = \sqrt{\frac{1}{T}\sum_{t=1}^{T}(Max(De_{i,t} - (Rp_{i,t} + Bo_{i,t} + Sf_{i,t} + Sg_{i,t} + \sum_{j=1}^{m}R_{i,j,t}), 0)^2} \tag{47}$$

where O denotes the total reservoir output.

The DRO is calculated for each reservoir with respect to non-violation of DT, meeting the water demands, and power generation equals the PPC as follows:

$$\overset{3}{\underset{r=1}{DRO_{i,r}}} = [1 - (\frac{RMSE_{rc} - Min_{c=1}^{4}(RMSE_{rc})}{Max_{c=1}^{4}(RMSE_{rc}) - Min_{c=1}^{4}(RMSE_{rc})})] \times 100 \tag{48}$$

in which $r = 1,2,3$ and $c = 1,2,3$ denote the number of rows and columns of the matrix P, respectively.

4. Assigning weights to the reservoir-operation objectives

This study assigns weights to each reservoir's and the multi-reservoir system's objectives. This work applies the weighted least squares method (Chu et al., 1979), which assigns criteria weights based on the expertise of decision-makers (Bozorg-Haddad et al., 2021b). The readers can find more details about the weighted least squares method in Chu et al. (1979) and Bozorg-Haddad et al. (2021b).

5. Case study

The Karkheh basin was chosen as a case study to illustrate this paper's methodology. This basin is located in southwestern Iran. Fig. 5 shows the location of the Karkheh Basin. Karkheh river is formed by the confluence of the Seimare and Kashkan rivers and discharges to the Hoor-al-Azim wetland. The length of the main branch of the Karkheh river from its Gamasiab source to the Hoor-al-Azim wetland is 875 km. The Seimare and Karkheh reservoirs are the operating reservoirs in the basin. Table 1 lists the technical specifications of the reservoirs. The experience of a decade of drought in Iran led to development within the Seimare river floodplain. Spillway gates were installed in the Seimare reservoir's dams prior to 2018–2019 and 2019–2020 that could have

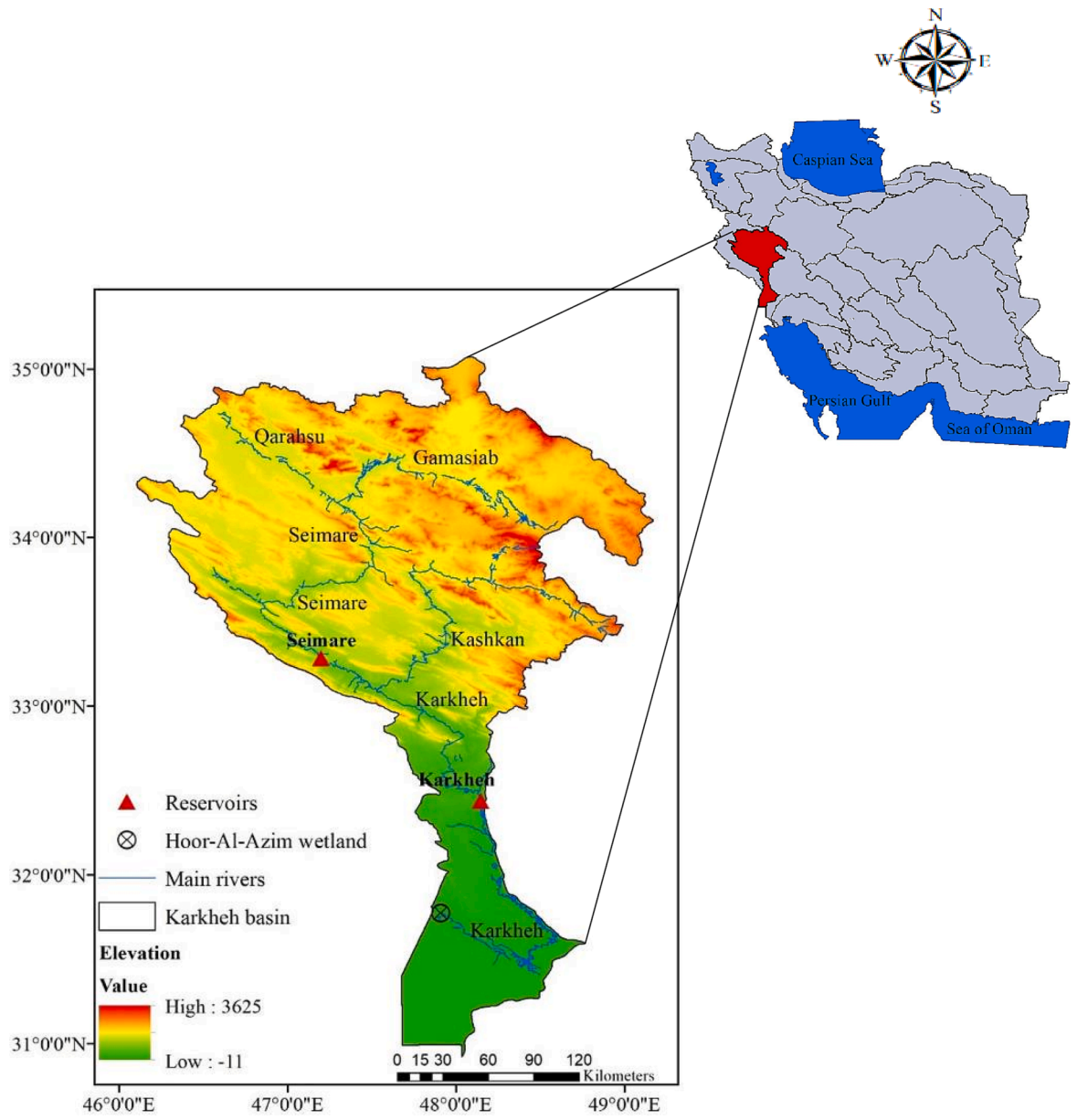

Fig. 5. Location of the study area in Iran (ArcGIS 10.8.1).

reduced flood damages (Bozorg-Haddad, 2019). The Abbas plain gate is located on Karkheh reservoir's right side to meet the Abbas plain's agricultural water demands.

Iran experienced three major waves of extreme precipitation in Mar. and Apr. 2019, which caused severe floods in different parts of that country (Zarei et al., 2021a). The southwestern basins, including the Karkheh basin, endured the largest share of the second and third waves of precipitation in Mar. 24–26 and Mar. 31-Apr. 2, respectively, which inflicted heavy losses to life and property (Aminyavari et al., 2019). Also, in Mar. and Apr. 2020, small and medium floods inflicted losses at various locations. Fig. 6.a and 6.b confirm the distinct magnitude of inflows in 2018–2019 and 2019–2020 for Seimare and Karkheh reservoirs in accordance with Iranian months. This work evaluated the performance of the Seimare and Karkheh reservoirs during the 2019 and 2020 floods. The knowledge to be gained from this study's forensic analysis of the performance of the reservoirs will contribute to the mitigation of future flood damages by means of reservoir operation.

6. Results and discussion

The SOP and IA were applied in this study for the forensic assessment of the performance of the Seimare and Karkheh reservoirs in achieving multiple objectives during the 2019 and 2020 floods. According to Bozorg-Haddad (2019), for the two-reservoir system and Karkheh reservoir meeting demands has the most importance followed by flood control and hydropower generation, respectively. However, flood control, meeting downstream demands and hydropower generation have been respectively considered more important for the Seimare reservoir, as its downstream demands involve only the Seimare river's environmental demands (see Table 1). In this regard, the weights assigned to flood control, meeting water demands, and hydropower generation for the two-reservoir system are 35, 45 and 20%, for the Seimare reservoir are 51, 30 and 19% and for the Karkheh reservoir are 40, 45 and 15%, respectively (Bozorg-Haddad, 2019).

The Seimare and Karkheh reservoir inflows in the flood years are presented in Fig. 6c and d. It is seen in Fig. 6c and d that floods in the

Table 1
The technical specifications of the Seimare and Karkheh reservoirs.

	Reservoirs	
	Seimare	Karkheh
River	Seimare river	Karkheh river
Type	Double arched concrete	Soil with clay core
Objectives	Meeting the environmental demands, flood control and hydropower generation	Meeting the environmental, industrial, agricultural and drinking demands, flood control and hydropower generation
Spillway type	Free & Gated	Gated
Normal water level (masl)	723	220
Water level of maximum operation (masl)	723	226
Spill threshold level (masl)	704.5	209
Minimum water level (masl)	680	170
Crown level (masl)	730	234
Bottom outlet levels (masl)	620 & 640	110
Abbas plain gate level (masl)	–	175
Minimum water level for power plant performance (masl)	693	185
Installed power plant capacity (Mw)	480	400
No downstream damage threshold (m^3/s)	250	400
Considerable downstream damage threshold (m^3/s)	620	1000

Karkheh basin occurred in Jan. 21-Feb. 19, Feb. 20-Mar. 20, Mar. 21-Apr. 20 and Apr. 21-May. 21. The SOP and IA were developed since Nov. 22-Dec. 21 in 2018–2019 and 2019–2020 to be provided a sufficient time for reservoirs pre-release. The MPPC corresponding to the Seimare and Karkheh reservoirs were set equal to 95 and 97%, respectively, for both the SOP and IA due to the long-term readiness of the power plant units.

6.1. *Forensic assessment of the multi-reservoir system performance under floods in 2018–2019*

The SOP and IA were implemented daily in the flood months to increase the accuracy of reservoir management. Fig. 7 shows the initial storage and water releases for the Seimare reservoir corresponding to the HM, SOP, and IA in 2018–2019. Fig. 8 depicts the initial storage, water release (sum of the powerplant, bottom outlet and spillway releases), and releases from the Abbas plain gate for the Karkheh reservoir corresponding to the HM, SOP and IA in 2018–2019.

Several small and medium floods occurred before the floods of Mar. in addition to large floods in Jan. 21- Feb. 19 that impacted the reservoirs. However, cautious commands to maintain reservoir storage due to experiencing the decade of drought, such as not meeting (i) the environmental demands of the Seimare river in Sep. 23-Oct. 22 and Oct. 23-Nov. 21 (Fig. 7a), (ii) the downstream water demands of the Karkheh reservoir in Oct. 23 – Nov. 21 and Nov. 22– Dec. 21 (Fig. 8a), and (iii) the water demands of Abbas plain in Sep. 23– Oct. 22 to Jan. 21- Feb. 19 (Fig. 8b) caused limited free storage in the reservoirs in the face of catastrophic floods (Fig. 7b and Fig. 8c). The Karkheh reservoir was filled to 91% of its capacity during the floods of Jan. 21- Feb. 19. Yet, in the period Feb. 20-Mar. 20 only about 1% of the reservoir storage was released (Fig. 8a). Also, in Sep. 23– Oct. 22, hydropower generation was suspended in the Seimare reservoir (Table 2), and during Mar. 21–24 the Seimare reservoir releases were reduced compared to the previous month to prevent turning off the power plant (Fig. 7a). Other results corresponding to HM, SOP and IA are listed in Table 2.

6.1.1. *Flood control*

The performance of the Seimare and Karkheh reservoir system achieved with HM, the SOP, and IA is depicted in Fig. 9. It is seen in Fig. 9a that the objective of flood control had NDT with coefficients equal to 1.0, 1.5, and 2.0, and the CDT were considered to be DTs. The SOP, HM, and IA with respect to the 1.0× NDT case produced reliability equal to 0.76, 0.67, and 0.50, respectively, and resiliency equal to 0.023, 0.008, and 0.005, respectively, of the reservoir system (see Fig. 9a). However, HM has the highest vulnerability of the multi-reservoir system (it is equal to 4.76). The HM and the SOP with respect to the case 1.5× NDT achieved minimum and maximum reliability of the multi-reservoir system equal to 0.76 and 0.89, respectively. The minimum and maximum resiliency of the reservoirs system obtained with HM and IA are 0.035 and 0.164, respectively. The system's vulnerability corresponding to HM, the SOP, and IA has the highest value equal to 2.84, 2.65, and 0.21, respectively. It is seen in Fig. 9a that the IA, SOP, and HM corresponding to the 2.0× NDT case achieved the highest reliability equal to 0.95, 0.91, and 0.90, respectively, and resiliency equal to 0.50, 0.032, and 0.028, respectively, and the lowest vulnerability equal to 0.06, 1.74, and 1.88, respectively, of the reservoir system. The IA did not produce system output larger than the CDT in any of the time steps. Therefore, according to the CDT, the IA has reliability, resiliency and vulnerability 1.0, 1.0, and 0, respectively. The SOP and HM have the highest reliability (0.93 and 0.91, respectively) after that of IA, and have the lowest vulnerability (1.19 and 1.31, respectively) for the multi-reservoir system. However, according to CDT the resiliency of the reservoir system is higher for HM (equals 0.059) compared to the SOP (equals 0.042).

The results show that according to the 2.0× NDT case and the CDT the reservoir system's performance criteria for IA with respect to flood control are better than the SOP's and HM's. The IA implements pre-releasing water from the reservoirs system timely and accepting the risk of minor damages before the large floods, rendering it better prepared for flood mitigation compared to the SOP and HM. This means the IA released water from the reservoirs system over a longer period with discharges between 1.0× NDT and 1.5× NDT compared to SOP and HM (but with lower vulnerability than HM and SOP) due to the lower reliability and resiliency of the reservoir system achieved with IA compared to SOP and HM according to the 1.0× NDT case. Besides, IA released the reservoirs system in a longer period with discharges between 1.5× NDT and 2.0× NDT compared to the SOP (but with lower vulnerability than the SOP) due to lower reliability of the reservoirs system for IA compared to SOP according to the 1.5× NDT case.

6.1.2. *Meeting water demands*

It is seen in Fig. 9b that HM has minimal reliability and resiliency (0.59 and 0.006, respectively) in the Seimare and Karkheh reservoirs system. The SOP and IA have equal reliability and resiliency (equal to 0.83 and 0.017, respectively). The vulnerability of the reservoir system is equal to 0.34 with respect to HM, the SOP, and IA.

6.1.3. *Hydropower generation*

Spillway gates were not installed in the Seimare reservoir in 2018–2019. Therefore, the reservoir could not generate hydropower to the extent of PPC that year. Moreover, this study assumed the MPPC to be lower than 100% for the Seimare and Karkheh reservoirs in the SOP and IA. Therefore, HM, the SOP, and IA produced failure from the perspective of hydropower generation for the multi-reservoir system in all the time steps of the water year. Therefore, the reliability of the reservoir system in generating hydropower with HM, the SOP, and IA is

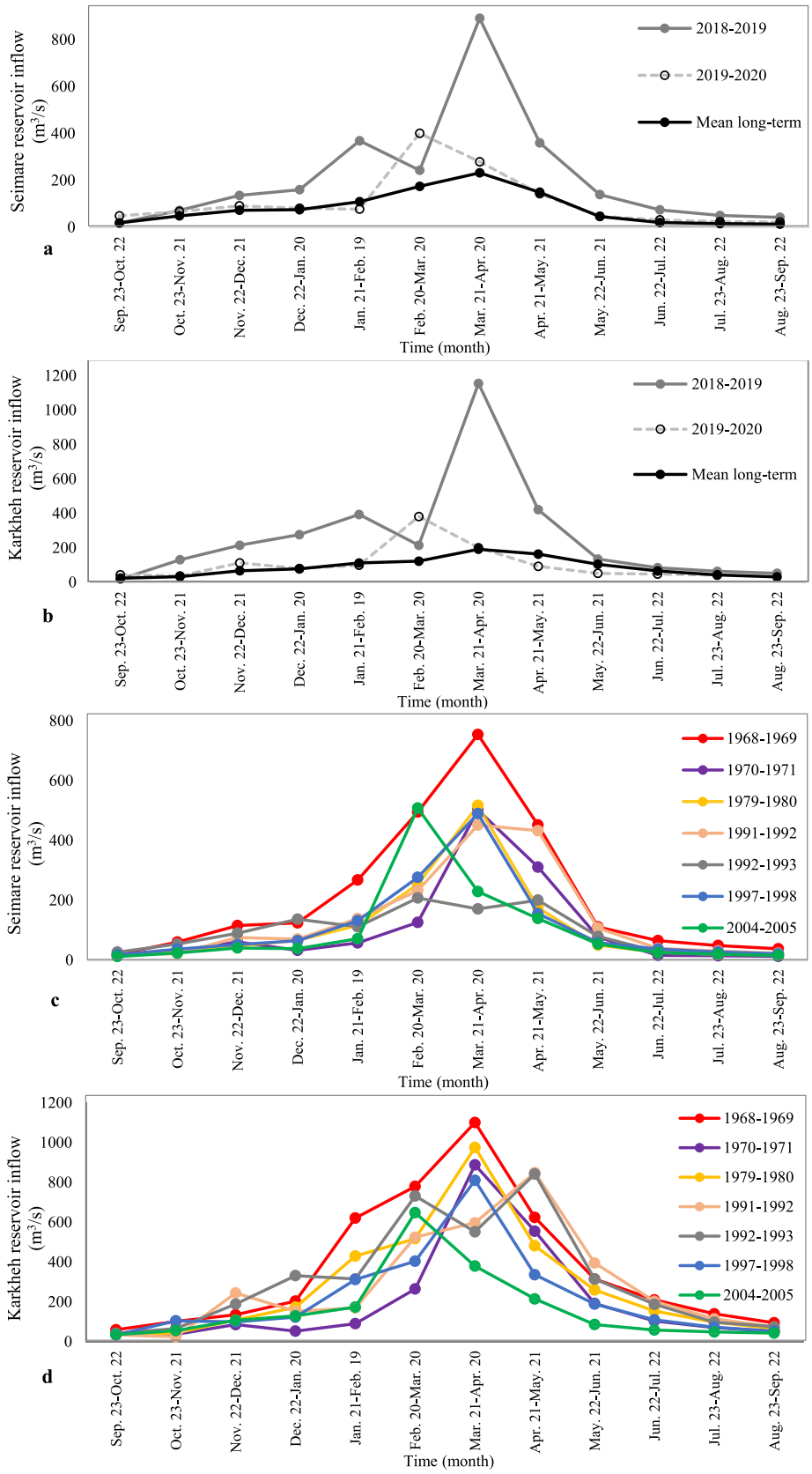

Fig. 6. Reservoirs' inflow; a and b. in 2018–2019 and 2019–2020 compared to the mean long-term, c and d. in flood years.

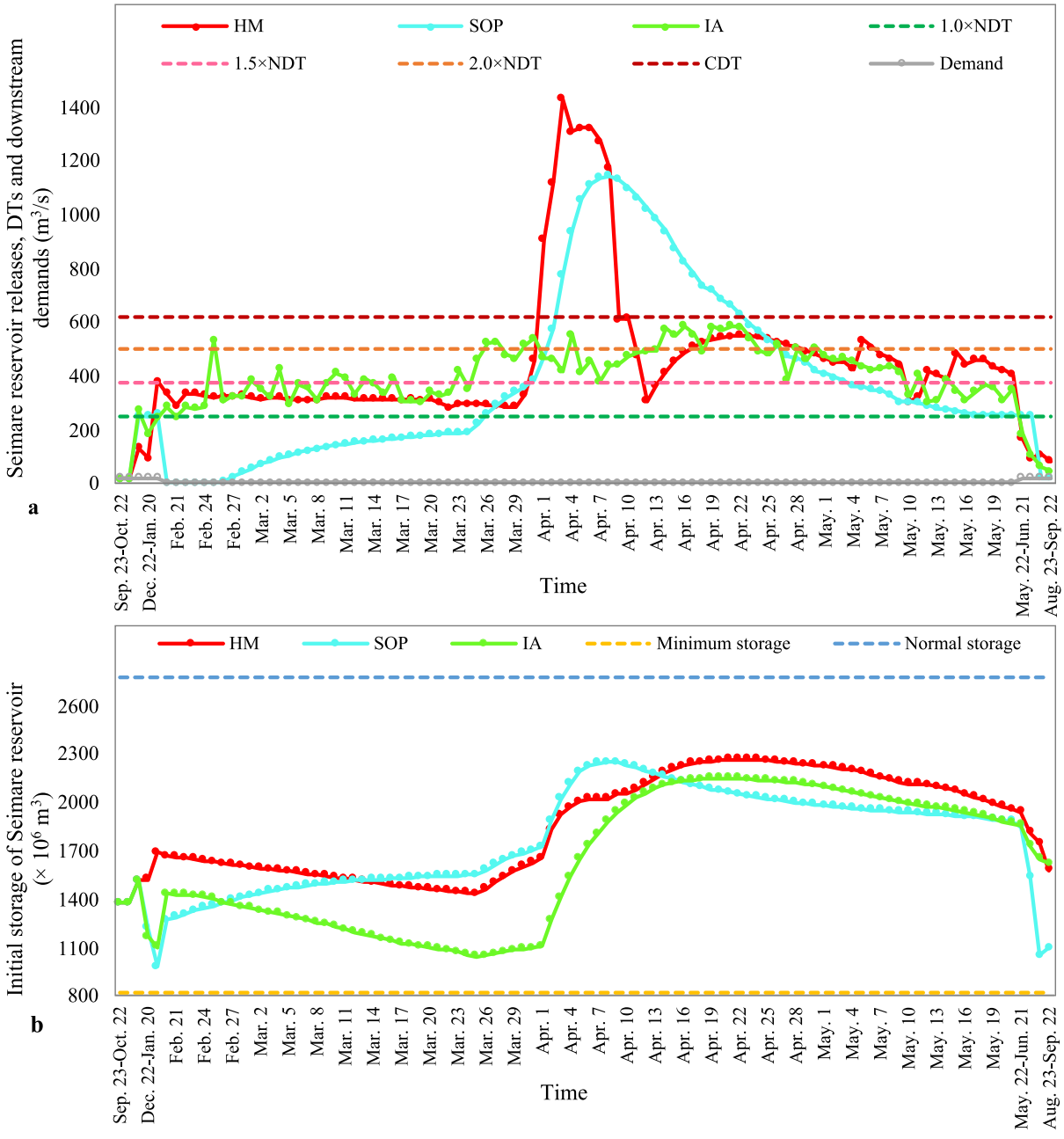

Fig. 7. Results of Seimare reservoir operation in 2018–2019 for the HM, SOP and IA.a. The reservoir release compared to the DTs and downstream demands, b.Initial storage of the resrvoir.

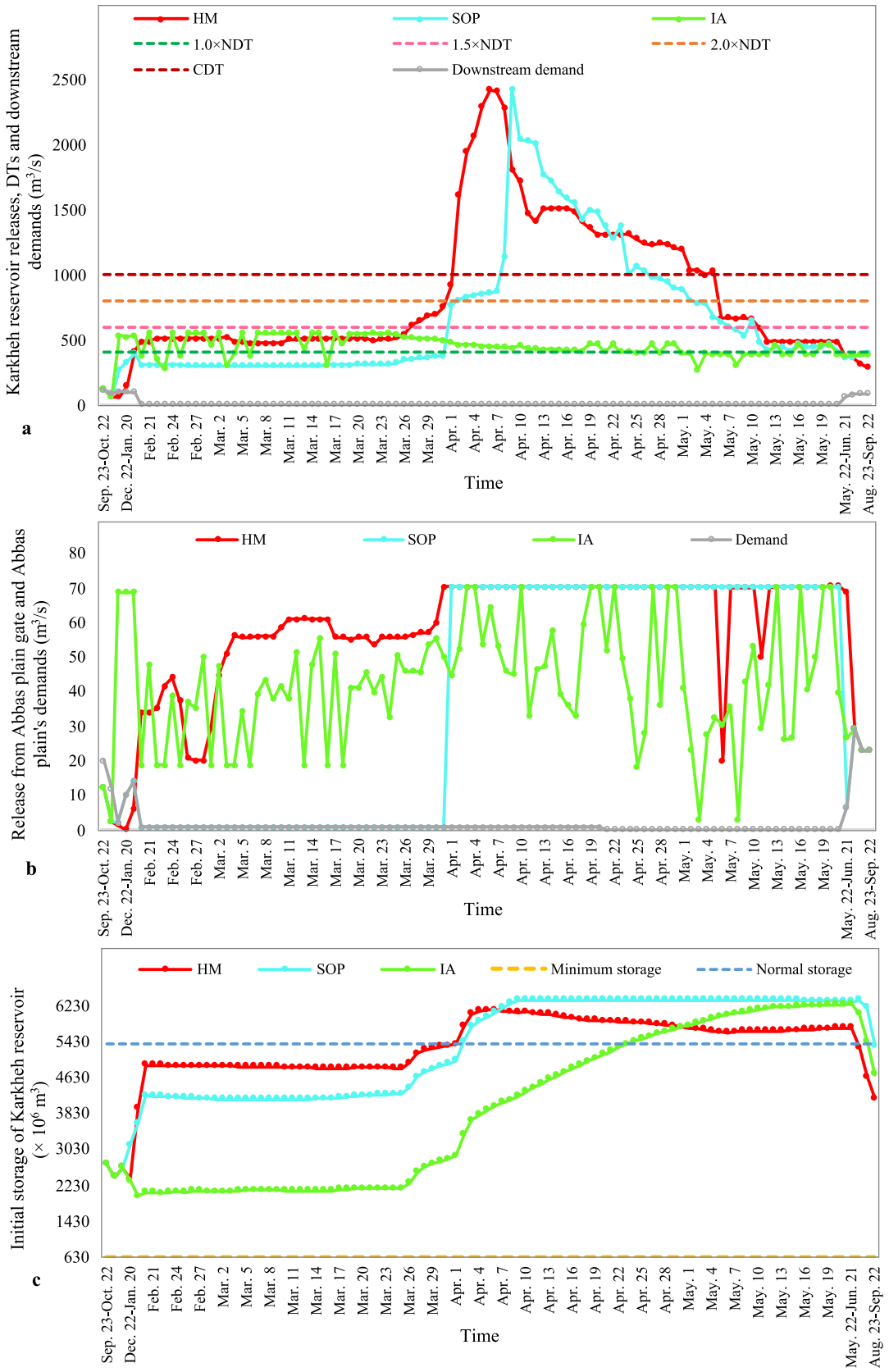

Fig. 8. Results of Karkheh reservoir operation in 2018–2019 for the HM, SOP and IA. a. The reservoir release (sum of the releases from the power plant, spillway, and bottom outlet) compared to the DTs and downstream demands; b. Release from Abbas plain gate compared to Abbas plain's water demands, c. Initial storage of the reservoir.

Table 2
The results of the HM, SOP, and IA in 2018–2019.

	Seimare reservoir			Karkheh reservoir		
	HM	SOP	IA	HM	SOP	IA
Time steps with powerplant turned off	Sep. 23– Oct. 22, Apr. 12–22, May. 1–2	Sep. 23– Oct. 22, Feb. 20–25, Jul. 23-Aug. 22, Aug. 23– Sep. 22	Sep. 23– Oct. 22, Feb. 27-Apr. 1	Apr. 5–23	–	–
The time step of closing one of the spillway chutes with a stop log	Since Apr. 2 to beginning of May. 22-Jun. 21	Since Apr. 1 to beginning of May. 22-Jun. 21	Since Apr. 7 to beginning of May. 22-Jun. 21	–	–	–

equal to 0. It is seen in Fig. 9c that the resiliency of the reservoirs system for HM, the SOP, and IA is equal (0.003). In comparison, the highest system's vulnerability values with respect to hydropower generation (0.75, 0.58 and 0.52) correspond to the HM, IA and SOP, respectively.

Fig. 10 displays the performance criteria of the Seimare and Karkheh reservoirs system by applying the objectives' weights. Table 3 establishes the superiority of the reservoir system's performance criteria calculated with SOP and IA compared to HM according to the DTs. Implementation of the SOP in 2018–2019 according to the 1.0× NDTcase would improve the reservoir system's reliability, resiliency, and vulnerability by 28, 167 and 7%, respectively. It is seen in Table 3 that the 1.5× NDT case with SOP achieves reservoir system's reliability, resiliency, and vulnerability criteria equal to 30, 69 and 9%, respectively, better than with HM. The 2.0× NDT case with HM produces inferior operation of the Seimare and Karkheh reservoirs system compared to the SOP. With HM the reliability, resiliency, and vulnerability of the reservoir system are 19, 46 and 10%, respectively, worse than the SOP's. The CDT with SOP produce reliability and vulnerability (equal to 18 and 10%, respectively) of the reservoir system that are better than the HM's. In contrast, the resiliency of the reservoirs system for HM is 4% superior to the SOP's (see Table 3).

The superior performance criteria for IA are established with respect to optimal flood control when the future reservoir inflows are known. Fig. 10 and Table 3 show that the operation of the multi-reservoir system by SOP is less different from the IA compared to HM. The best improvements of reliability, resiliency, and vulnerability obtained with IA in comparison with HM are equal to 26.5, 1408.5, and 76%, respectively. They correspond respectively to the 1.5× NDT, CDT, and 1.0× NDT cases.

6.2. Forensic assessment of the Seimare reservoir's performance under floods in 2018–2019

Fig. 11 displays the results of the forensic evaluation of HM's performance in the operation of the Seimare reservoir. The protection of unspoiled lands upstream (ULU) of Seimare reservoir along with flood control and reduction of downstream damages were the objectives of Seimare reservoir operation in 2018–2019. Fig. 11.a indicates that the maximum waterlogged area of ULU with HM (equals 56.8×10^6 m^2) is greater than those obtained with the SOP and IA (55.4×10^6 and 48.1×10^6 m^2, respectively). Therefore, IA and the SOP have better performance in protecting the Seimare reservoir's upstream lands than HM.

Fig. 11b indicates that HM and IA have the maximum and minimum RMSEs for violation of the DTs, respectively. For the RMSE corresponding to the IA and CDT is equal to 0. It is evident that values larger than 0 for RMSEs for the IA according to the 1.0× NDT, 1.5× NDT and 2.0× NDT cases is due to the lack of sufficient capacity in the Seimare reservoir to store floods. The Seimare reservoir could not play a considerable role in reducing flood discharges and downstream damages due to the lack of installation of spillway gates in 2018–2019. It is seen in Fig. 11b that the RMSE for HM and the SOP (135 and 134.5 m^3/s, respectively) have the lowest difference according to the 1.5× NDT case. The maximum difference between the RMSEs for SOP and HM (93 and 80 m^3/s, respectively) is associated with the CDT, which indicates better performance of the SOP in operating the Seimare reservoir to mitigate floods than with HM. Fig. 11c indicates that the RMSE values for not-meeting the downstream demands are equal for HM, the SOP, and IA (it is equal 0.4 m^3/s). Fig. 11d shows the minimum RMSE for violation of generating the PPC being associated with the SOP (it is equal 349 MW). In comparison, the IA has a maximum RMSE for violation of generating the PPC (it is equal 372 MW) due to turning off the power plant in 34 days by IA before the Mar. 31-Apr. 2 precipitation wave to increase the free storage in the Seimare reservoir.

Fig. 11e shows that if SOP were implemented in the Seimare reservoir the reservoir performance would be improved by 20, 17, 20 and 24% in achieving the objectives according to the 1.0× NDT, 1.5× NDT, 2.0× NDT and CDT, respectively. Fig. 11 indicates that the IA's performance in the Seimare reservoir operation is better than HM's and the SOP's according to all the DTs. The minimum difference with the Seimare reservoir performance for IA is associated with the SOP. The Seimare reservoir operation with SOP according to 1.0× NDT, 1.5× NDT, 2.0× NDT and CDT differs by 28, 31, 28 and 24%, respectively, from the IA, while according to all the DTs HM is 48% less desirable for the Seimare reservoir operation compared to IA.

6.3. Forensic assessment of the Karkheh reservoir's performance under floods in 2018–2019

Fig. 12 displays the results of the forensic evaluation of HM's performance in the operation of the Karkheh reservoir. Fig. 12a indicates that the IA exhibits the best performance in Karkheh reservoir operation for flood control according to all the DTs. The HM also has the worst performance in the Karkheh reservoir operation for all the DTs. The IA produces RMSEs for the violation of 1.5× NDT, 2.0× NDT and CDT equal to 0. According to 1.0× NDT the IA has an RMSE larger than 0 (equal to 78 m^3/s) in operation of the Karkheh reservoir due to the inability of its upstream reservoir (Seimare reservoir) to effectively control floods and assist the Karkheh reservoir due to the lack of installation of spillway gates. Fig. 12b shows that the maximum RMSE (equal to 3 m^3/s) for not-meeting the water demands of the Abbas plain corresponds to HM, while the SOP and IA have equal RMSE for not-meeting the demands (equal to 2 m^3/s). Fig. 12c shows that the minimum RMSE for not generating the PPC corresponds to IA (equal to 147 MW), and HM has the maximum RMSE (equal to 229 MW) for not generating the PPC. The 1.0× NDT and 2.0× NDT cases lead to Karkheh reservoir operation with HM that is 66 and 69% worse than the SOP, respectively (see Fig. 12d and e). Karkheh reservoir operation with HM is 65% worse compared to the SOP according to 1.5× NDT and CDT (see Fig. 12f and g). Suiadee and Tingsanchali (2007) found that applying the classic SOP in operation of the Nam Oon Reservoir in Thailand increases the total flood loss compared to the present reservoir operation. Sahu and McLaughlin (2018) found that the classic SOP sacrifices hydropower generation more than the Perfect Information Strategy approach when

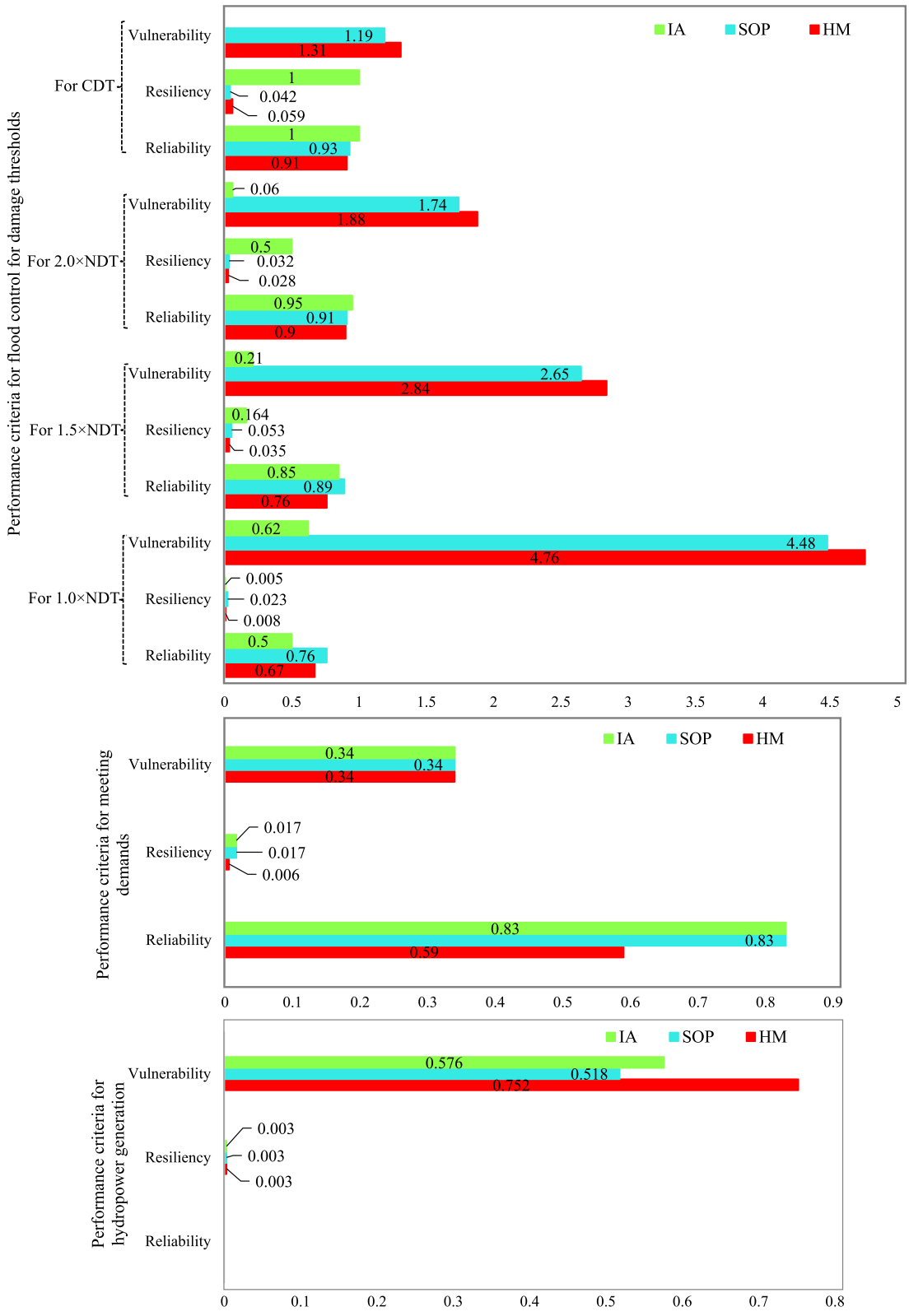

Fig. 9. Performance criteria for the multi-reservoir system for objectives in 2018–2019. a. flood control, b. meeting water demands and c. hydropower generation.

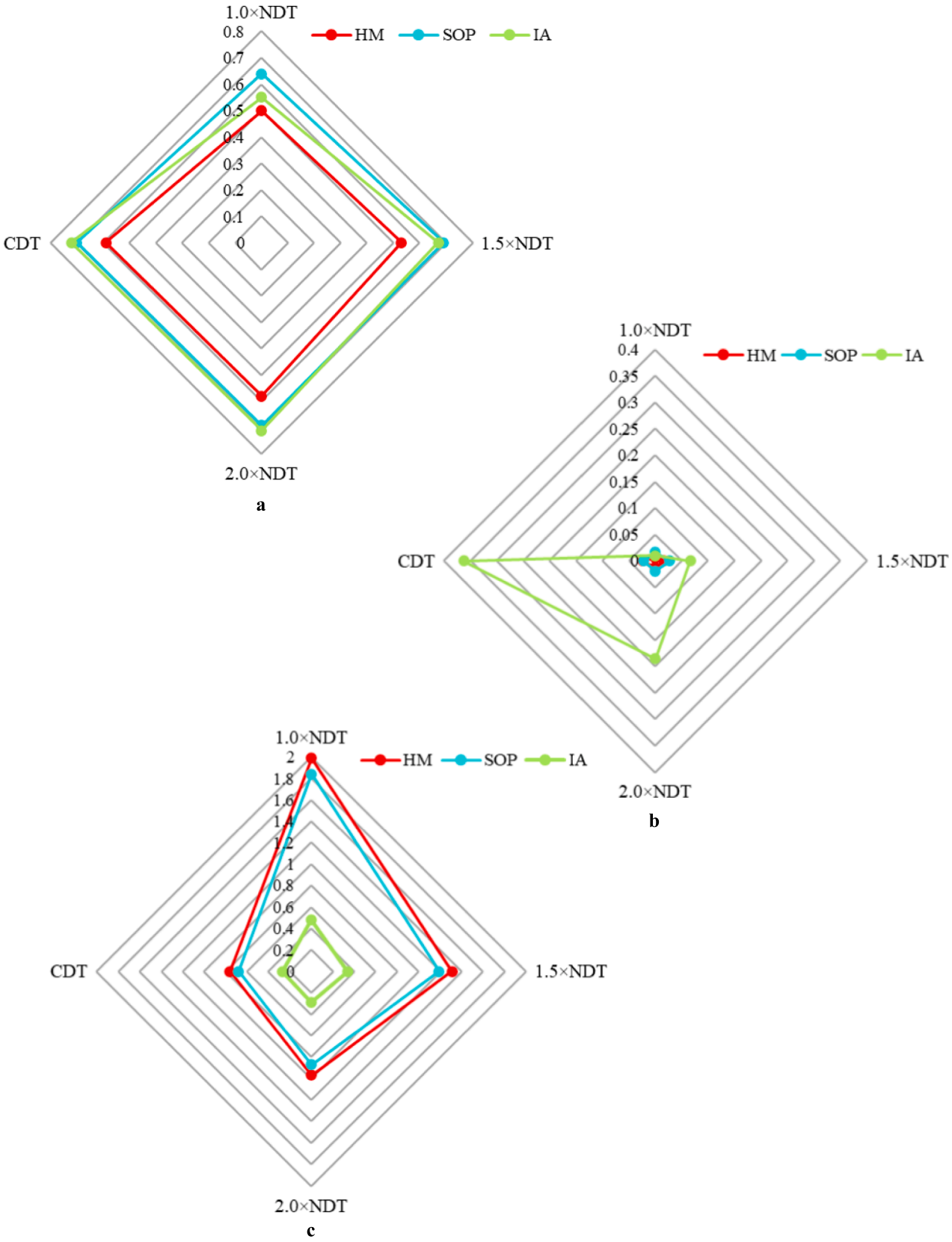

Fig. 10. Performance criteria for the Seimare and Karkheh reservoirs system in 2018–2019; a. reliability, b. resiliency and c. vulnerability.

Table 3
The superiority percentage of the Seimare and Karkheh reservoirs system's performance criteria for the SOP and IA compared to the HM in 2018–2019.

The DTs	Performance criteria	The superiority of approaches to the HM (%)	
		SOP	IA
1.0 × NDT	Reliability	28	10
	Resiliency	167	67
	Vulnerability	7.5	76
1.5 × NDT	Reliability	30	26.5
	Resiliency	69	312.5
	Vulnerability	9	74
2.0 × NDT	Reliability	19	22.5
	Resiliency	46	1323
	Vulnerability	10.5	70
CDT	Reliability	18.5	22
	Resiliency	−4	1408.5
	Vulnerability	10.5	64.5

spills are penalized.

This paper's results show that the IA exhibits maximum desirability with respect to Karkheh reservoir operation. Fig. 12 indicates that for all the DTs the IA is 100% better than HM. Comparison of the DRO values established that according to 1.0× NDT and 2.0× NDT the IA is 34 and 31% better for operating Karkheh reservoir, respectively, than the SOP. Also, according to 1.5× NDT and CDT the SOP is 35% worse than the ideal management of the Karkheh reservoir.

Appendix A shows the results of the forensic assessment of reservoir operation in 2019–2020.

7. Sensitivity analysis of the forensic assessment results with respect to the objectives' weights for the 2019 flood

Table 4 and Fig. 13 include changes in average superiority of the SOP and IA over HM in response to changes in objectives' weights for the Seimare and Karkheh reservoirs. It is seen that increasing the weight of flood control for the Seimare and Karkheh reservoirs reduces the superiority of the SOP to HM (see Fig. 13.a). However, the larger the weight of hydropower generation, the higher the superiority of the SOP over HM. Table 4 shows that if the weight of meeting hydropower demand were 100%, the superiority of the SOP over HM would be 0 and 100% for the Seimare and Karkheh reservoirs, respectively. Moreover, the inferiority of HM with respect to the SOP would be accentuated by operating both reservoirs with equal weights.

It is seen that for Seimare reservoir, flood control's and hydropower generation's weights are the most sensitive weights for superiority of IA to HM (see Table 4). According to Fig. 13a, increasing flood control's weight and reducing hydropower generation's weight raises superiority of IA than HM for the Seimare reservoir. However, the IA's superior operation over HM for the Karkheh reservoir is not sensitive to the objectives' weights (see Fig. 13b).

8. Conclusion

This study proposed a framework for the forensic assessment of reservoir operation performance during floods. The SOP was introduced for multi-objective reservoirs considering practical operational rules. The performance of the Seimare and Karkheh reservoirs under the framework achieved with the SOP and IA during the floods of 2019 and 2020 was evaluated and compared with the historic management (HM). The results showed that in 2018–2019, on average, the reliability, resiliency, and vulnerability of the multi-reservoir system obtained with HM were worse by 25, 34 and 9%, respectively, compared to the SOP, and by 20, 954 and 72%, respectively, compared to IA. In 2019–2020, on average, the reliability, resiliency, and vulnerability of the reservoirs system obtained with HM would improve with the SOP by 33, 233, and 40%, respectively, and with the IA it would improve by 34, 279 and 46%, respectively. The key impediment to mitigating the 2019 flood was the lack of operational spillway gates in the Seimare reservoir. The limited capacity of the Seimare reservoir prevents the IA and SOP from protecting against flood damages downstream. Despite the catastrophic floods of 2019 the spillway gates were not installed in 2020. The results obtained with the IA indicate that the key to the significant mitigation of damages caused by the 2019 floods was efficient pre-release of water from the reservoirs and sacrificing hydropower generated by the Seimare reservoir. However, cautious flood-control actions during flooding resulted in insufficient water releases with the intention to preserve storage to meet downstream water demands later in the summer. Closing one of the Seimare reservoir's spillway chutes by a stop log was an optimal measure taken under HM and SOP, as IA chooses this option to increase the reservoir's capacity. The application of the SOP and IA revealed that in 2020 the operators over released water ahead of the floods from the Karkheh reservoir given the destruction caused by floods the previous year.

This study's results show that the SOP's operational policies can potentially improve the reservoir's performance in achieving flood-control objectives. The desirable performance of reservoirs under SOP during 2019 and 2020 floods shows that the proposed forensic framework can be applied for evaluating reservoir operation of reservoirs during floods.

9. Limitations of the study and further research

Despite the valuable results gained from the forensic assessment of reservoir operation in this study there remain limitations. This study assumes that the amount of leakage from the reservoirs is 0. Also, flood routing is not performed in the rivers. Therefore, a cautious stance must be taken when comparing the SOP and IA with HM by assuming that the total water release from the upstream reservoirs is transferred to the downstream reservoirs. This work does not consider water-quality parameters in reservoir operation, which could impact turbine

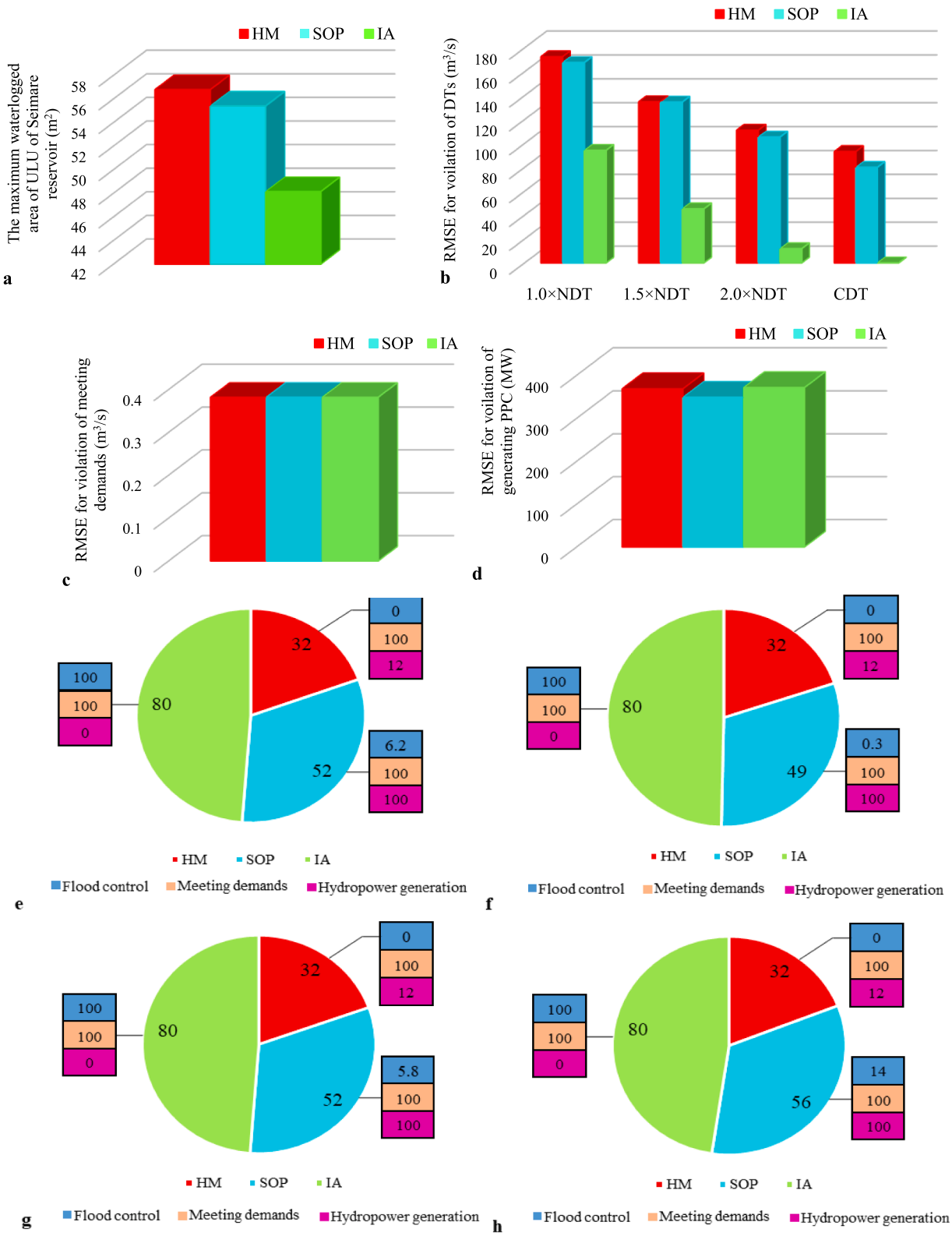

Fig. 11. The results of forensic assessment of Seimare reservoir for HM, SOP and IA in 2018–2019. a. The maximum waterlogged area of the ULU of the reservoir; b. RMSEs for violation of the DTs; c. RMSEs for not-meeting demands; d. RMSEs for violation of generation of the PPC; e, f, g and h. DROs by applying objectives' weight according to 1.0 × NDT, 1.5 × NDT, 2.0 × NDT and CDT, respectively.

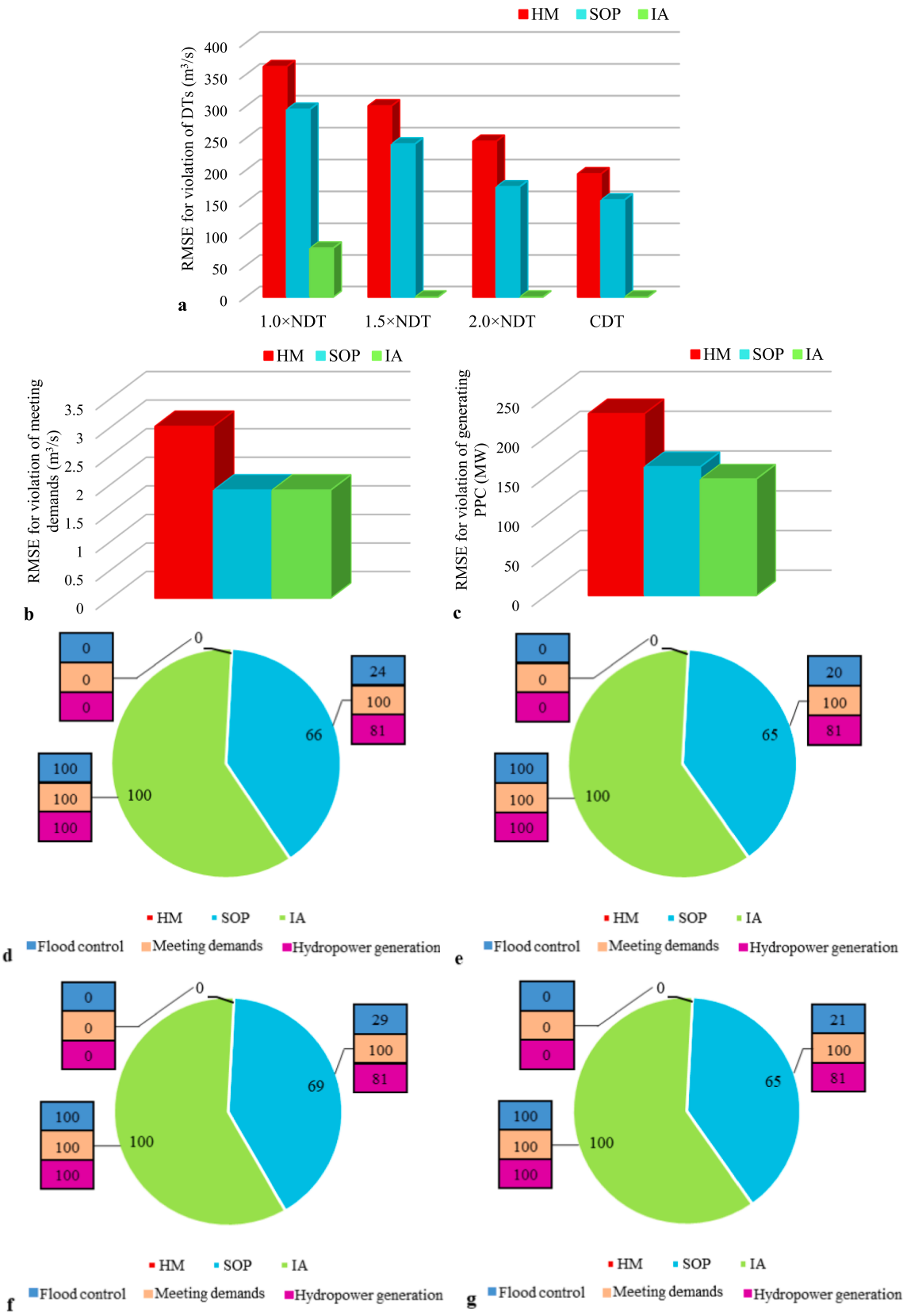

Fig. 12. The results of forensic assessment of Karkheh reservoir for HM, SOP and IA in 2018–2019. a. RMSEs for violation of the DTs; b. RMSEs for not-meeting demands; c. RMSEs for violation of generation of the PPC; d, e, f and g. DROs by applying objectives' weight according to 1.0 × NDT, 1.5 × NDT, 2.0 × NDT and CDT, respectively.

Table 4
Sensitivity analysis of the forensic assessment results to objectives' weights of the reservoirs for the 2019 flood.

Reservoirs	Objective's weights (%)			The average superiority of SOP to the HM (%)	The average superiority of IA to the HM (%)
	Flood control	Meeting demands	Hydropower generation		
Seimare	51	30	19	20	48
	100	0	0	7	100
	0	100	0	0	0
	0	0	100	88	−12
	33.3	33.3	33.3	31	29
	45	33	22	22	42
Karkheh	40	45	15	66	100
	100	0	0	23	100
	0	100	0	100	100
	0	0	100	81	100
	33.3	33.3	33.3	68	100
	35	47	18	70	100

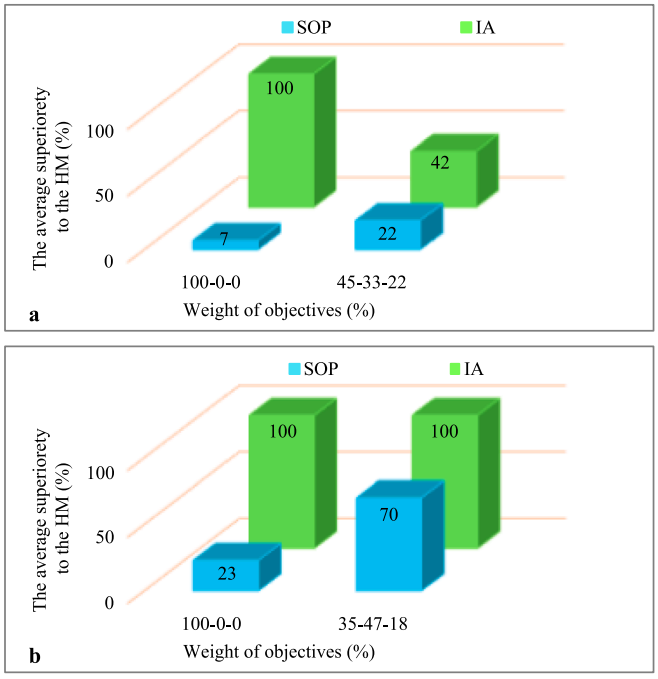

Fig. 13. Sensitivity analysis of the forensic assessment results to objectives' weights of the reservoirs for 2019 flood (The weights are related to flood control, meeting demands, and hydropower generation, respectively); a. Seimare reservoir, b. Karkheh reservoir.

performance. Moreover, especial conditions could change the assumptions made for assigning the priorities of opening reservoir gates made in this study. For instance, if none of the powerplant units is functional, reservoirs could not generate hydropower. Also, suspended sediment invading the power plant's power tunnel may stop hydropower generation. Under these circumstances the opening of the gates allowing water into the turbines does not take precedence among the reservoir gates. Each of these limitations could be addressed in future studies. Future studies comparing the HM with the SOP and IA under the assumption of spillway gates being installed in the Seimare reservoir before floods would be valuable. Furthermore, developing forensic engineering criteria considering the damage to property would be desirable in future research.

CRediT authorship contribution statement

Manizhe Zarei: Software, Formal analysis, Writing – original draft. **Omid Bozorg-Haddad:** Conceptualization, Supervision, Project administration. **Hugo A. Loáiciga:** Validation, Writing – review & editing.

Declaration of Competing Interest

The authors declare that they have no known competing financial interests or personal relationships that could have appeared to influence the work reported in this paper.

Data availability

No data was used for the research described in the article.

Acknowledgements

The authors acknowledge Iran's National Science Foundation (INSF) support for this research, and are indebted to Hossein Aghamohamady, a Water and Energy expert and operator and designer of dams for its assistance, gathering data, supporting and training Manizhe Zarei regarding hydrology, floods, and flood attenuation by means of reservoir operation.

Appendix A. The forensic assessment results of HM under the 2019-2020 floods.

Forensic assessment of the multi-reservoir system performance under flood conditions in 2019-2020

It is shown in Figs. 5c and d that the maximum inflows to Seimare and Karkheh reservoirs occurred in 20 Feb-20 Mar, 21 Mar-20 Apr and 21 Apr-21 May. However, due to the downward trend of the reservoirs' inflow since late Mar. 21-Apr. 20 the SOP and IA were implemented daily only in Feb. 20-Mar. 20 and Mar. 21-Apr. 20 in 2019-2020. Appendix B presents the initial storage and release values for the Seimare reservoir with HM, the SOP, and IA in 2019-2020. Appendix C presents the initial storage, release (sum of the powerplant, bottom outlet and spillway releases) and release from Abbas plain gate for the Karkheh reservoir with HM, the SOP, and IA in 2019-2020. The reservoirs faced increasing inflow trends in the early days of Feb. 20-Mar. 20 compared to previous months (see Figs. 5a and b). However, the storage of Seimare reservoir increased in Feb. 21-25 (before floods) to prevent turning off the power plant (see Appendix B) even though predictions indicated floods in Feb. 20-Mar. 20 and warnings were also issued for the evacuation of the floodplain. The HM produced Karkheh reservoir water releases in excess NDT in 25 days (see Appendix C), while the reservoir had a great deal of free storage to store floods. Appendix D presents the results corresponding to HM, SOP and IA.

Flood control

Appendix E presents the performance criteria values for the objectives of the multi-reservoir system. It is seen in Appendix E.a that the IA, HM and SOP have the highest reliability (0.96, 0.89 and 0.88, respectively) and resiliency (0.66, 0.08 and 0.05, respectively) for reservoir system, respectively according to the 1.0×NDT case. In contrast, the highest vulnerability (0.47, 0.27, 0.01,) of the system correspond to the HM, SOP, and IA, respectively. The reliability, resiliency and vulnerability of the reservoir system corresponding to the IA are 1, 1 and 0, respectively, according to the 1.5×NDT case, because the reservoir system's output was not more than the 1.5×NDT case in any of the time steps of the water year. After IA the maximum reliability and resiliency and the minimum vulnerability (0.99, 0.33 and 0.05, respectively) correspond to the SOP. The reservoir system's output in the water year corresponding to the HM, SOP, and IA does not exceed 2.0×NDT and the CDT, which means that their reliability, resiliency and vulnerability are equal to 1, 1 and 0, respectively.

Meeting water demands

The HM has minimum reliability and resiliency and maximum vulnerability (0.57, 0.025 and 0.08, respectively) for the multi-reservoir system. It is seen in Appendix E.b that the SOP and IA meet the water demands in all the time steps by reservoir operation.

Hydropower generation

The period 2019-2020, as it was in the previous year, was a failure in terms of not generating the PPC according to the HM, the SOP, and IA due to the lack of installation of spillway gates in the Seimare reservoir. Therefore, the reservoirs system's reliability for HM, SOP and IA is equal to 0. According to Appendix E.c the HM, IA, and SOP have the highest vulnerability (0.66, 0.59 and 0.58, respectively), while the resiliency is equal for all of them (equals 0.003).

Appendix F depicts the reservoirs system's performance criteria by applying the objectives' weight. According to the 1.0×NDT case the reliability, resiliency, and vulnerability of reservoir operation corresponding to the HM are 33, 1061.5 and 50.5% worse than the SOP, respectively. The reservoir system performance corresponding to the HM is 36, 1194.5 and 36.5% worse than the SOP in terms of reliability, resiliency and vulnerability, respectively, according to the 1.5×NDT case. According to the 2.0×NDT case and the CDT reservoir operation performance corresponding to the SOP in 2019-2020 would be 31.5, 119, and 31%, better with respect to the reliability, resiliency, and vulnerability, respectively, than the HM's.

Appendix F demonstrates the superior performance obtained with the IA compared to the HM and SOP. It is seen in Appendix F the SOP's reservoir-operation performance is closer to the IA's than HM's.

Forensic assessment of the Seimare reservoir's performance under flood conditions in 2019-2020.

Appendix G presents the results of the forensic evaluation of the Seimare and Karkheh reservoirs' performance in 2019-2020 with the HM, SOP and IA. Appendix G.a indicates that the HM's performance in protecting the lands upstream of the Seimare reservoir is worse than the SOP and IA. The waterlogged area of ULU of the Seimare reservoir obtained with HM, SOP, and IA are 9.6×10^6, 6.7×10^6 and 0 m^2, respectively.

It is seen in Appendix G.b and 7.c that with 1.0×NDT and 1.5×NDT the HM's performance in Seimare reservoir operation is 49 and 63% worse than with SOP, respectively. The 2.0×NDT and CDT operation of the Seimare reservoir with HM is 18% worse than with the SOP (see Appendix G.d and e).

These paper's results show that IA's DROs is 100% effective in achieving the objectives of the Seimare reservoir according to all the DTs. Based on the 1.0×NDT, 1.5×NDT, 2.0×NDT and CDT the SOP's performance is 21, 7, 1 and 1%, respectively, different from the ideal performance associated with IA in the Seimare reservoir. The performance of Seimare reservoir operation with HM according to 1.0×NDT, 1.5×NDT, and 2.0×NDT and CDT is 70, 70, 19 and 19% is inferior in comparison with IA.

Forensic assessment of the Karkheh reservoir's performance under flood conditions in 2019-2020

Appendix G.f shows that according to the 1.0×NDT case the SOP could have improved the Karkheh reservoir performance by 100% in achieving the operational objectives. According to other DTs the desirability of Karkheh reservoir performance with HM is 60% lower than with the SOP.

The DRO values show that according to all DTs the desirability of Karkheh reservoir operation for SOP and IA from the perspective of flood control and meeting water demands is 100% due to the lack of violation of the reservoirs' outputs with respect to the DTs and meeting demands in all time steps. The managerial desirability of IA from hydropower generation is 17% lower than SOP due to less generated hydropower for IA compared to the SOP in 2019-2020. As a result, according to all DTs, Karkheh reservoir's DROs for IA is 3% lower compared to SOP. According to the results, in comparison with HM, the performance deviation of Karkheh reservoir for IA is 97% according to 1.0×NDT and 57% according to other DTs.

Sensitivity analysis of the forensic assessment results to objectives' weights for the 2019-2020 flood.

The results of sensitivity analysis to investigate the impact of objectives' weights on superiority of SOP and IA to HM are found in Appendixes H and I. Concerning the Seimare reservoir the most effective weight for superiority of SOP and IA to HM corresponds to hydropower generation (see Appendix I.a), followed by flood control's and meeting demand's weights, respectively. For the Karkheh reservoir, increasing meeting demand's and hydropower generation's and reducing flood control's weight raises the superiority of the SOP over HM (see Appendix I.b). Furthermore, the superiority of the reservoirs' operation under SOP and IA would increase in response to equal weights for the objectives.

Appendix B. Results of Seimare reservoir operation in 2019-2020 for the HM, SOP and IA; a. The reservoir release compared to DTs and downstream demands, b.Initial reservoir storage.

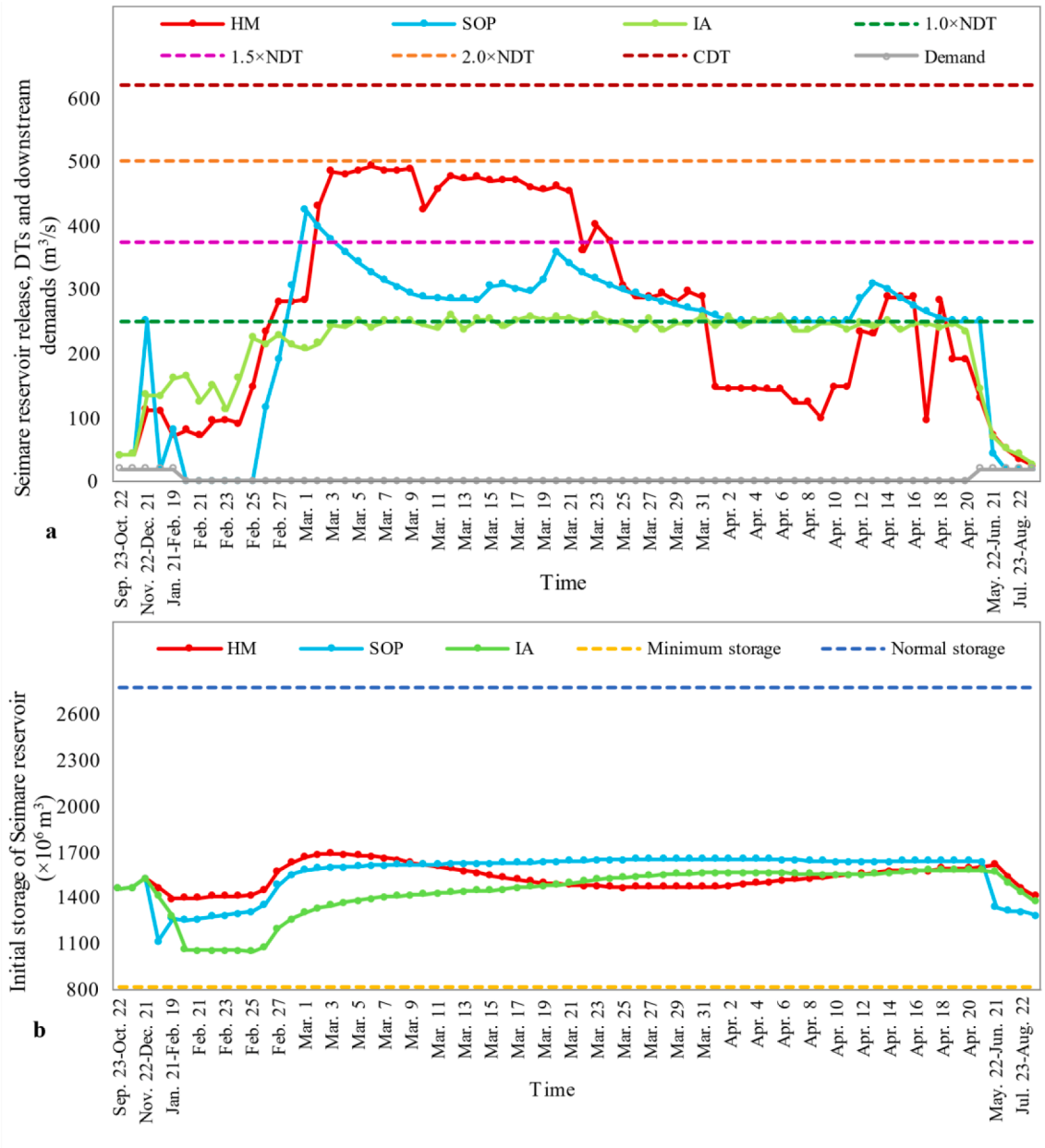

Appendix C. Results of Karkheh reservoir operation in 2019-2020 for the HM, SOP and IA; a. The reservoir release compared to DTs and downstream demands; b. Release from Abbas plain gate compared to Abbas plain's demands, c.Initial reserovoir storage.

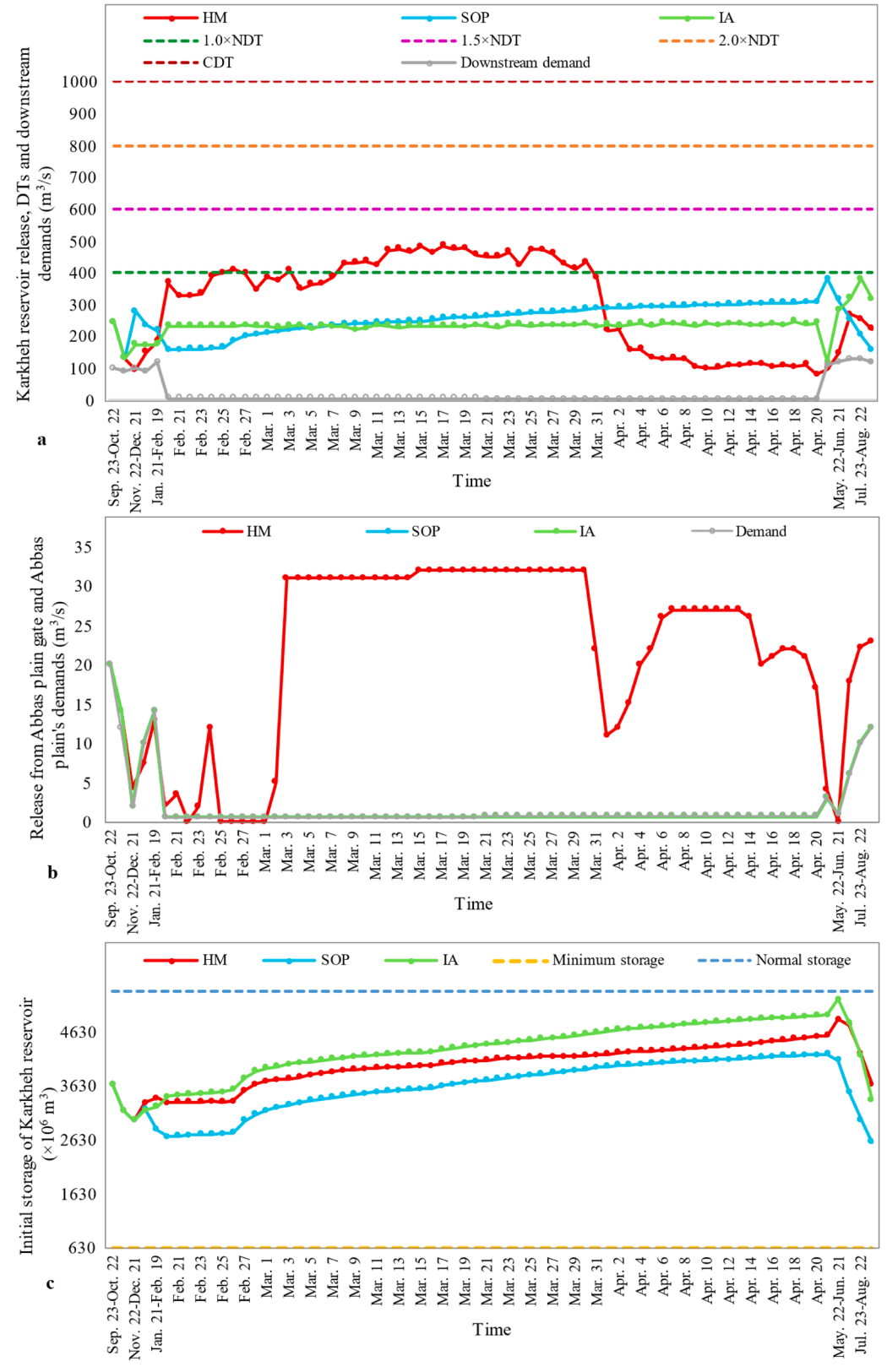

Appendix D. The results of the HM, SOP, and IA in 2019-2020.

	Seimare reservoir			Karkheh reservoir		
	HM	SOP	IA	HM	SOP	IA
Time steps with powerplant turning off	-	Dec. 22-Jan. 20, Feb. 20-25, Jun. 22-July. 22, July. 23-Aug. 22, Aug. 23-Sep. 22	Feb. 20-Mar. 2	-	-	-

Appendix E. Performance criteria for the multi-reservoir system for objectives in 2019-2020; a. flood control, b. meeting water demands and c. hydropower generation

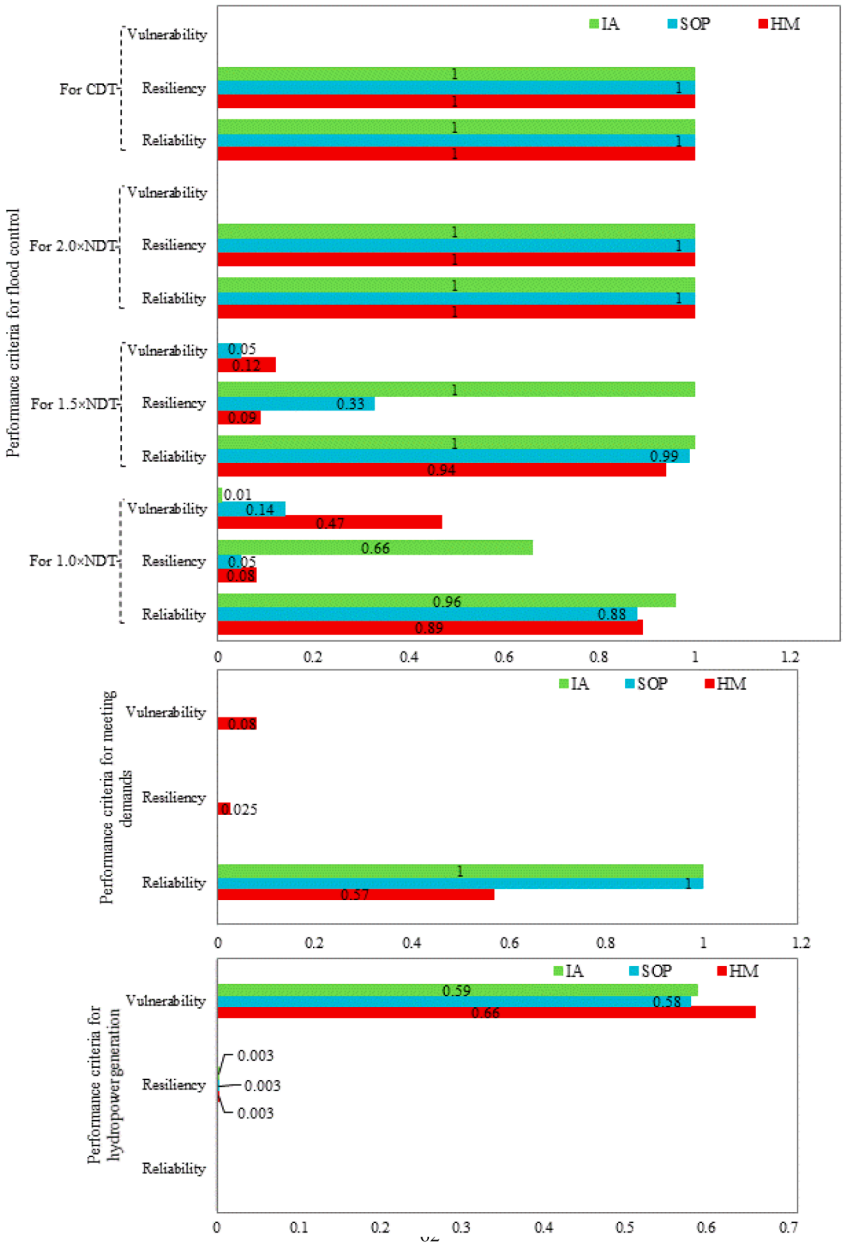

Appendix F. Performance criteria for the Seimare and Karkheh reservoirs system in 2019-2020; a. reliability, b. resiliency and c. vulnerability.

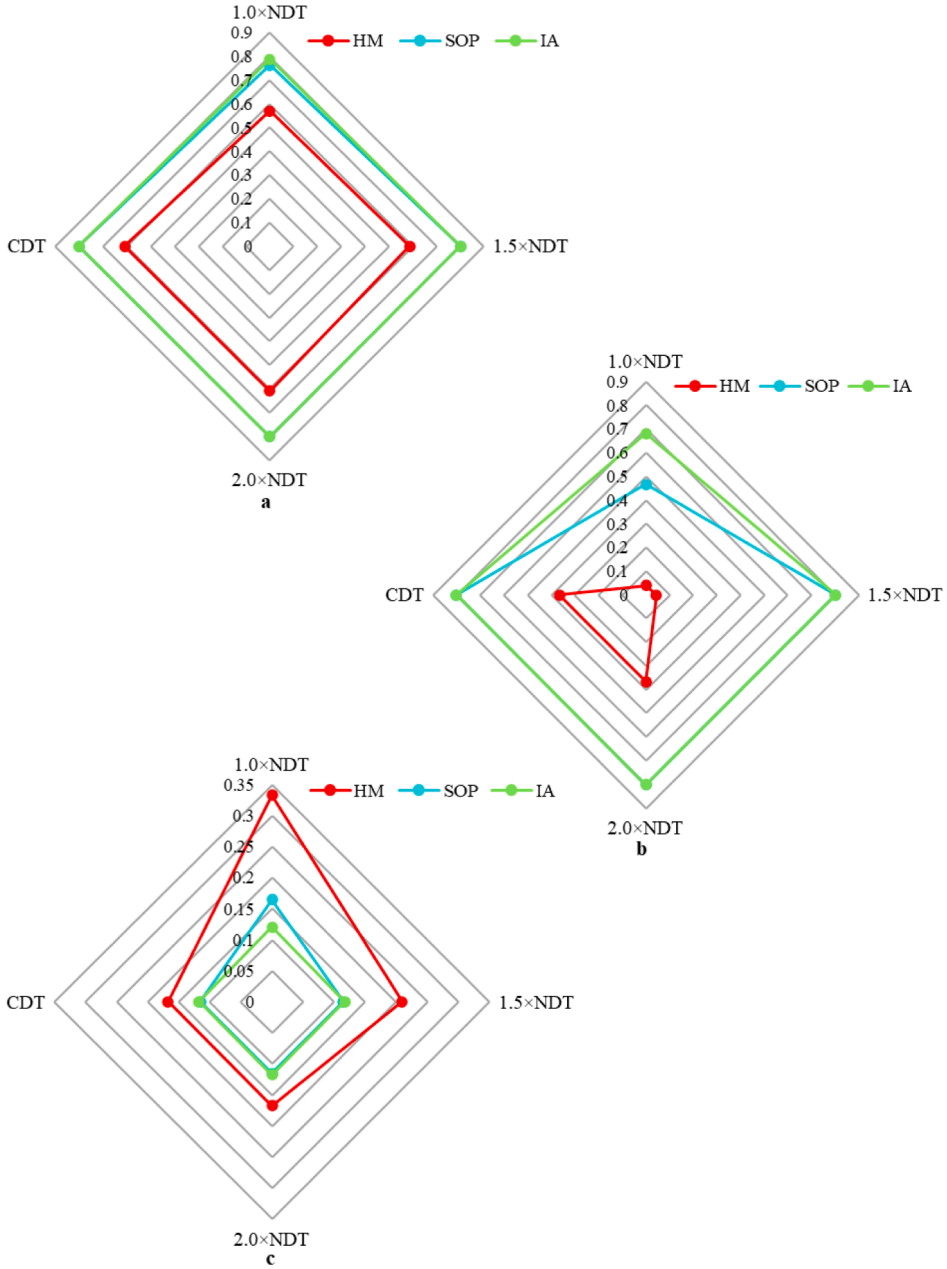

Appendix G. The results of forensic assessment the reservoirs' performance for the HM, SOP and IA in 2019-2020; a. The maximum waterlogged area of the ULU of the Seimare reservoir; b, c, d and e. Seimare reservoir's DRO by applying objectives' weight according to 1.0×NDT, 1.5×NDT, 2.0×NDT and CDT, respectively; f, g, h and i. Karkheh reservoir's DRO by applying objectives' weight according to 1.0×NDT, 1.5×NDT, 2.0×NDT and CDT, respectively.

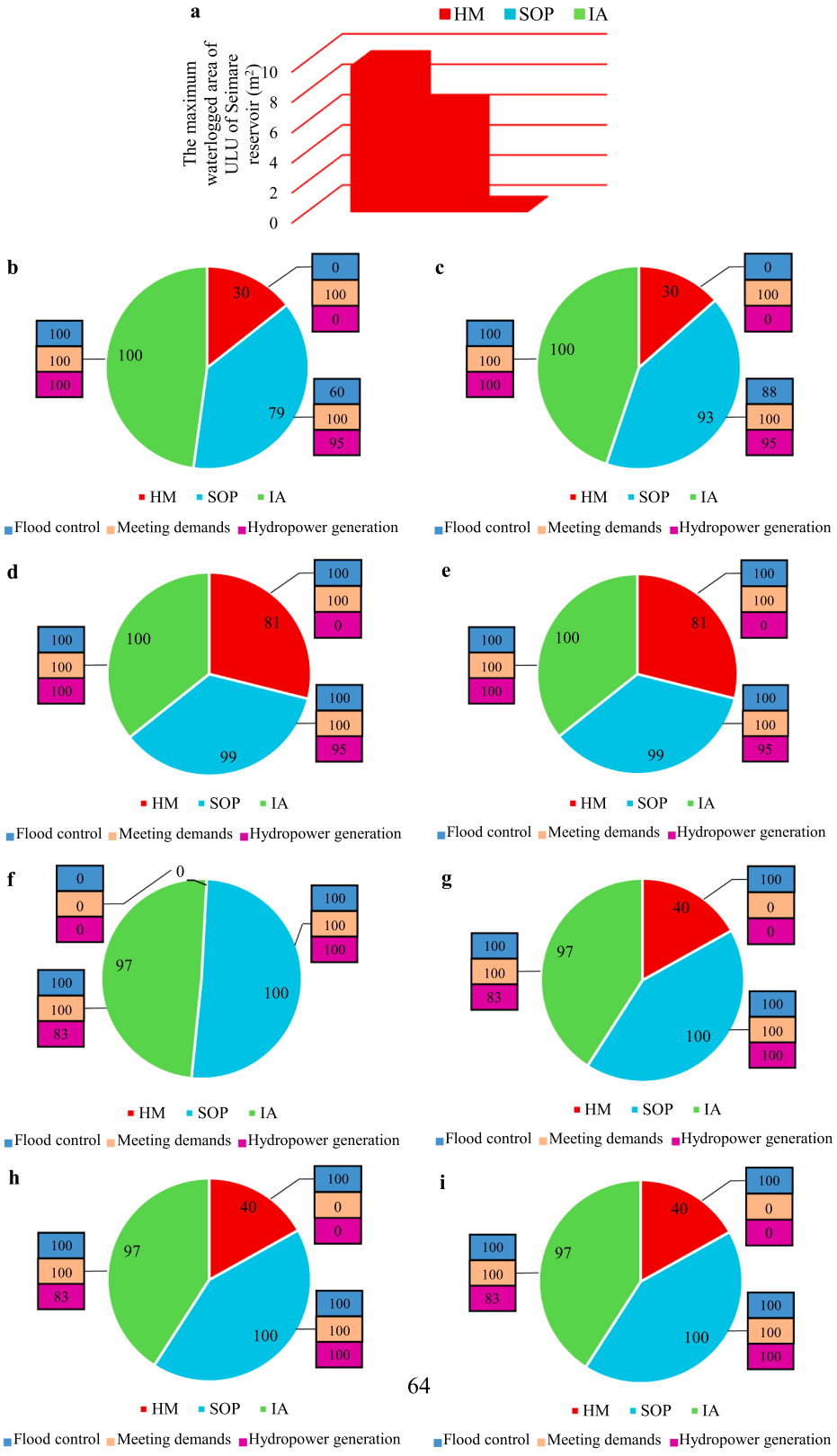
a
HM SOP IA
The maximum waterlogged area of ULU of Seimare reservoir (m²)
0 2 4 6 8 10
b
30 100 79
0 100 0
100 100 100
60 100 95
HM SOP IA
Flood control Meeting demands Hydropower generation
c
30 100 93
0 100 0
100 100 100
88 100 95
HM SOP IA
Flood control Meeting demands Hydropower generation
d
81 100 99
100 100 0
100 100 100
100 100 95
HM SOP IA
Flood control Meeting demands Hydropower generation
e
81 100 99
100 100 0
100 100 100
100 100 95
HM SOP IA
Flood control Meeting demands Hydropower generation
f
0 97 100
0 0 0
100 100 100
100 100 83
HM SOP IA
Flood control Meeting demands Hydropower generation
g
40 97 100
100 0 0
100 100 83
100 100 100
HM SOP IA
Flood control Meeting demands Hydropower generation
h
40 97 100
100 0 0
100 100 83
100 100 100
HM SOP IA
Flood control Meeting demands Hydropower generation
i
40 97 100
100 0 0
100 100 83
100 100 100
HM SOP IA
Flood control Meeting demands Hydropower generation

64

Appendix H. Sensitivity analysis of the forensic assessment results to objectives' weights of the reservoirs for 2020 flood.

Reservoirs	Objective's weights (%)			The average superiority of SOP to the HM (%)	The average superiority of IA to the HM (%)
	Flood control	Meeting demands	Hydropower generation		
Seimare	51	30	19	37	45
	100	0	0	37	50
	0	100	0	0	0
	0	0	100	95	100
	33.3	33.3	33.3	44	50
	56	23	21	41	49
Karkheh	40	45	15	70	67
	100	0	0	25	25
	0	100	0	100	100
	0	0	100	100	83
	33.3	33.3	33.3	75	69
	43	40	17	68	65

Appendix I Sensitivity analysis of the forensic assessment results to objectives' weights of the reservoirs for 2020 flood (The weights are related to flood control, meeting demands, and hydropower generation, respectively); a. Seimare reservoir, b. Karkheh reservoir.

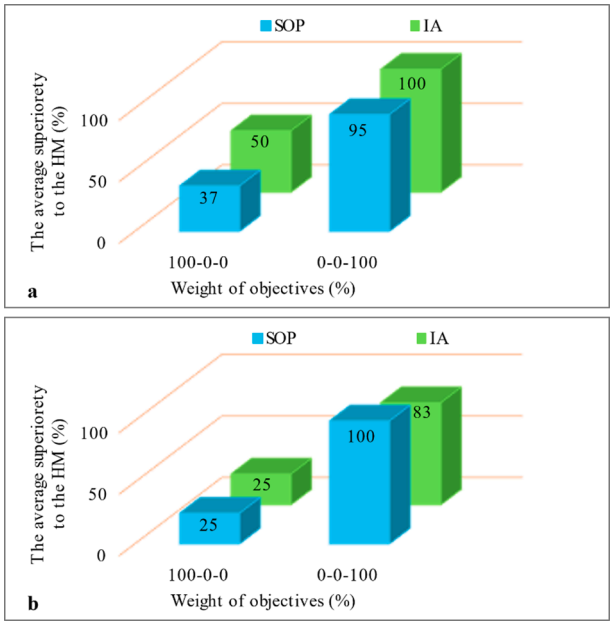

References

Abdi, B., Bozorg-Haddad, O., Chu, X., 2021. Uncertainty analysis of model inputs in riverine water temperature simulations. Sci. Rep. 11, 1–14.

Ahmadianfar, I., Samadi-Koucheksaraee, A., Bozorg-Haddad, O., 2017. Extracting optimal policies of hydropower multi-reservoir systems utilizing enhanced differential evolution algorithm. Water Resour. Manag. 31 (14), 4375–4397.

Akbari-Alashti, H., Bozorg Haddad, O., Fallah-Mehdipour, E., Mariño, M.A., 2014. Multi-reservoir real-time operation rules: A new genetic programming approach, Proceedings of the institution of civil engineers-water management. Proceedings of the Institution of Civil Engineers - Water Management 167 (10), 561–576.

Aminyavari, S., Saghafian, B., Sharifi, E., 2019. Assessment of precipitation estimation from the NWP models and satellite products for the spring 2019 severe floods in Iran. Remote Sens. 11, 2741.

Bahrami, M., Bozorg-Haddad, O., Chu, X., 2018. Cat Swarm Optimization (CSO) Algorithm. In: Bozorg-Haddad, O. (Ed.), Advanced Optimization by Nature-Inspired Algorithms. Springer Singapore. Singapore. 9-18. DOI:10.1007/978-981-10-5221-7_2.

Boulange, J., Hanasaki, N., Yamazaki, D., Pokhrel, Y., 2021. Role of dams in reducing global flood exposure under climate change. Nat. Commun. 12, 1–7.

Bozorg-Haddad, O., 2019. Investigation of floods in 2019 from the perspective of reservoir management. Special Committee on National Flood Report, Karaj, Iran.

Bozorg-Haddad, O., Ashofteh, P.-S., Mariño, M., 2015. Levee Layouts and Design Optimization in Protection of Flood Areas. J. Irrig. Drain. Eng. http://dx.doi.org/10.1061/(ASCE)IR.1943-4774.0000864. DOI:10.1061/(ASCE)IR.1943-4774.0000864.

Bozorg-Haddad, O., Janbaz, M., Loáiciga, H.A., 2016. Application of the gravity search algorithm to multi-reservoir operation optimization. Adv. Water Resour. 98, 173–185.
Bozorg-Haddad, O., Mariño, M.A., 2011. Optimum operation of wells in coastal aquifers, Proceedings of the Institution of Civil Engineers-Water Management. Proceedings of the Institution of Civil Engineers - Water Management 164 (3), 135–146.
Bozorg-Haddad, O., Moradi-Jalal, M., Mirmomeni, M., Kholghi, M.K., Mariño, M.A., 2009. Optimal cultivation rules in multi-crop irrigation areas. Irrig. and Drain. 58 (1), 38–49.
Bozorg-Haddad, O., Soleimani, S., Loáiciga, H.A., 2017. Modeling water-quality parameters using genetic algorithm–least squares support vector regression and genetic programming. J. Environ. Eng. 143, 04017021.
Bozorg-Haddad, O., Zolghadr-Asli, B., Chu, X., Loáiciga, H.A., 2021a. Intense extreme hydro-climatic events take a toll on society. Nat Hazards 108 (2), 2385–2391.
Bozorg-Haddad, O., Zolghadr-Asli, B., Loáiciga, H.A., 2021b. A handbook on multi-attribute decision-making methods. John Wiley & Sons.
Bronstert, A., Agarwal, A., Boessenkool, B., Crisologo, I., Fischer, M., Heistermann, M., Köhn-Reich, L., López-Tarazón, J.A., Moran, T., Ozturk, U., Reinhardt-Imjela, C., Wendi, D., 2018. Forensic hydro-meteorological analysis of an extreme flash flood: The 2016–05-29 event in Braunsbach. SW Germany. Sci. Total Environ. 630, 977–991.
Carper, K.L., 2000. Forensic engineering. CRC Press.
Chang, F.-J., Chen, L., 1998. Real-coded genetic algorithm for rule-based flood control reservoir management. Water resources management 12, 185–198.
Che, D., Mays, L.W., 2015. Development of an optimization/simulation model for real-time flood-control operation of river-reservoirs systems. Water Resources Management 29 (11), 3987–4005.
Chu, A.T.W., Kalaba, R.E., Spingarn, K., 1979. A comparison of two methods for determining the weights of belonging to fuzzy sets. J. Optim. Theory Appl. 27 (4), 531–538.
Connaughton, J., King, N., Dong, L., Ji, P., Lund, J., 2014. Comparing simple flood reservoir operation rules. Water 6, 2717–2731.
Delpasand, M., Fallah-Mehdipour, E., Azizipour, M., Jalali, M., Safavi, H.R., Saghafian, B., Loáiciga, H.A., Babel, M.S., Savic, D., Bozorg-Haddad, O., 2021. Forensic engineering analysis applied to flood control. J. Hydrol. 594, 125961.
Diakakis, M., Deligiannakis, G., Antoniadis, Z., Melaki, M., Katsetsiadou, N.K., Andreadakis, E., Spyrou, N.I., Gogou, M., 2020. Proposal of a flash flood impact severity scale for the classification and mapping of flash flood impacts. J. Hydrol. 590, 125452.
Dodangeh, E., Choubin, B., Eigdir, A.N., Nabipour, N., Panahi, M., Shamshirband, S., Mosavi, A., 2020. Integrated machine learning methods with resampling algorithms for flood susceptibility prediction. Sci. Total Environ. 705, 135983.
Fallah-Mehdipour, E., Bozorg Haddad, O., Beygi, S., Mariño, M.A., 2011. Effect of utility function curvature of Young's bargaining method on the design of WDNs. Water Resour. Manag. 25 (9), 2197–2218.
Golberg, D.E., 1989. Genetic algorithms in search, optimization, and machine learning. Addion wesley 1989 (102), 36.
Haghizadeh, A., Siahkamari, S., Haghiabi, A.H., Rahmati, O., 2017. Forecasting flood-prone areas using Shannon's entropy model. J. Earth Syst. Sci. 126, 1–11.
Harmancioğlu, N.B., 1994. Flood control by reservoirs, Coping with Floods. Springer, Dordrecht. 637-652.
Hashimoto, T., Stedinger, J.R., Loucks, D.P., 1982. Reliability, resiliency, and vulnerability criteria for water resource system performance evaluation. Water Resour. Res. 18 (1), 14–20.
Holland, J., 1975. Adaptation in natural and artificial systems. Ann Arbor.
Hossain, M., Nair, M., Mohd Sidek, L., Marufuzzaman, M., 2019. A pre-release concept for reservoir management and the effect analysis on flood control, International Conference on Dam Safety Management and Engineering. Springer. 556-566.
Huang, X., Xu, B., Zhong, P.-a., Yao, H., Yue, H., Zhu, F., Lu, Q., Sun, Y.u., Mo, R., Li, Z., Liu, W., 2022. Robust multiobjective reservoir operation and risk decision-making model for real-time flood control coping with forecast uncertainty. J. Hydrol. 605, 127334.
Karamouz, M., Imen, S., Nazif, S., 2012. Development of a demand driven hydro-climatic model for drought planning. Water Resour. Manag. 26 (2), 329–357.
Kim, T., Heo, J.H., Jeong, C.S., 2006. Multireservoir system optimization in the Han River basin using multi-objective genetic algorithms. Hydrological Processes: An International Journal 20 (9), 2057–2075.
Kong, D., Miao, C., Duan, Q., Li, J., Zheng, H., Gou, J., 2022. Xiaolangdi Dam: A valve for streamflow extremes on the lower Yellow River. J. Hydrol. 606, 127426.
Kumar, V., Yadav, S., 2020. Optimization of water releases from Ukai reservoir using Jaya Algorithm, Advanced Engineering Optimization Through Intelligent Techniques: Select Proceedings of AEOTIT 2018. Springer. 323-336.
Loáiciga, H.A., 2001. FLOOD DAMAGES IN CHANGING FLOOD PLAINS: A FORENSIC-HYDROLOGIC CASE STUDY. J. Am. Water Resour. Assoc. 37 (2), 467–478.
Louks, D.P., Sigvaldason, O.T., 1981. Multiple reservoir operation in North America. Surface Water Impoundments. ASCE 711–728.
Lund, J.R., Guzman, J., 1999. Derived operating rules for reservoirs in series or in parallel. J. Water Resour. Plan. Manag. 125 (3), 143–153.
Luo, J., Chen, C., Xie, J., 2015. Multi-objective immune algorithm with preference-based selection for reservoir flood control operation. Water Resour. Manag. 29 (5), 1447–1466.
Neelakantan, T., Sasireka, K., 2013. Hydropower reservoir operation using standard operating and standard hedging policies. Int. J. Eng. Technol. 5, 1191–1196.
Nilsson, C., Berggren, K., 2000. Alterations of riparian ecosystems caused by river regulation: Dam operations have caused global-scale ecological changes in riparian ecosystems. How to protect river environments and human needs of rivers remains one of the most important questions of our time. Biosci. 50, 783–792.
Noon, R.K., 2000. Forensic engineering investigation. CRC Press.
Sadeghi, M., Shearer, E.J., Mosaffa, H., Gorooh, V.A., Rahnamay Naeini, M., Hayatbini, N., Katiraie-Boroujerdy, P.-S., Analui, B., Nguyen, P., Sorooshian, S., 2021. Application of remote sensing precipitation data and the CONNECT algorithm to investigate spatiotemporal variations of heavy precipitation: Case study of major floods across Iran (Spring 2019). J. Hydrol. 600, 126569.
Sahu, R.K., McLaughlin, D.B., 2018. An Ensemble Optimization Framework for Coupled Design of Hydropower Contracts and Real-Time Reservoir Operating Rules. Water Resour. Res. 54 (10), 8401–8419.
Shrestha, B.B., Kawasaki, A., 2020. Quantitative assessment of flood risk with evaluation of the effectiveness of dam operation for flood control: A case of the Bago River Basin of Myanmar. Int. J Disaster Risk Reduct 50.
Soltanjalili, M., Bozorg-Haddad, O., Mariño, M.A., 2011. Effect of breakage level one in design of water distribution networks. Water Resour. Manag. 25 (1), 311–337.
Srinivasan, K., Philipose, M.C., 1996. Evaluation and selection of hedging policies using stochastic reservoir simulation. Water Resour. Manag. 10 (3), 163–188.
Srivastava, D.K., Awchi, T.A., 2009. Storage-yield evaluation and operation of Mula Reservoir. India. J. Water Resour. Plan. Manag. 135 (6), 414–425.
Suiadee, W., Tingsanchali, T., 2007. A combined simulation–genetic algorithm optimization model for optimal rule curves of a reservoir: a case study of the Nam Oon Irrigation Project. Thailand. Hydrol. Process. 21 (23), 3211–3225.
Tegegne, G., Kim, Y.-O., 2020. Representing inflow uncertainty for the development of monthly reservoir operations using genetic algorithms. Journal of Hydrology 586, 124876.
Van Pham, T., 2011. Tracking the uncertainty in streamflow prediction through a hydrological forecasting system, Master Civil Engineering and Management, University of Twente, NLD.
Yang, T., Zhang, L., Kim, T., Hong, Y., Zhang, D., Peng, Q., 2021. A large-scale comparison of Artificial Intelligence and Data Mining (AI&DM) techniques in simulating reservoir releases over the Upper Colorado Region. J. Hydrol. 602, 126723.
Yeh, W.-W.-G., 1985. Reservoir Management and Operations Models: A State-of-the-Art Review. Water Resour. Res. 21, 1797–1818. https://doi.org/10.1029/WR021i012p01797.
Zarei, M., Bozorg-Haddad, O., Baghban, S., Delpasand, M., Goharian, E., Loáiciga, H.A., 2021a. Machine-learning algorithms for forecast-informed reservoir operation (FIRO) to reduce flood damages. Sci. Rep. 11, 1–21.
M. Zarei O. Bozorg-Haddad V.P. Singh Forensic engineering O. Bozorg-Haddad Water Resources: Future Perspectives, Challenges, Concepts and Necessities 2021 IWA Publishing 287 314.
Zhao, T., Zhao, J., Lund, J.R., Yang, D., 2014. Optimal hedging rules for reservoir flood operation from forecast uncertainties. J. Water Resour. Plan, Manag, p. 140.
Zhou, Y., Guo, S., Liu, P., Xu, C., 2014. Joint operation and dynamic control of flood limiting water levels for mixed cascade reservoir systems. J. Hydrol. 519, 248–257.
Zolghadr-Asli, B., Bozorg-Haddad, O., Chu, X., 2019. Effects of the uncertainties of climate change on the performance of hydropower systems. J. Water Clim. Chang. 10, 591–609.